BOURLÈS BERNARD (ORCID ID: 0000-0001-6515-4519)
ARAUJO MOACYR (ORCID ID: 0000-0001-8462-6446)
MCPHADEN MICHAEL, J. (ORCID ID: 0000-0002-8423-5805)
BRANDT PETER (ORCID ID: 0000-0002-9235-955X)
FOLTZ GREGORY, R. (ORCID ID: 0000-0003-0050-042X)
LUMPKIN RICK (ORCID ID: 0000-0002-6690-1704)
GIORDANI HERVÉ (ORCID ID: 0000-0001-5517-2473)
HERNANDEZ FABRICE (ORCID ID: 0000-0003-2152-0657)
LEFÈVRE NATHALIE (ORCID ID: 0000-0002-1126-5528)
CAMPOS EDMO, J. D. (ORCID ID: 0000-0001-6399-5496)
DENGLER MARCUS (ORCID ID: 0000-0001-5993-9088)
HAHN JOHANNES (ORCID ID: 0000-0002-5638-2031)
ROUAULT MATHIEU (ORCID ID: 0000-0002-3207-6777)
SUTTON ADRIENNE, J. (ORCID ID: 0000-0002-7414-7035)
PEREZ RENELLYS, CHRISTINE (ORCID ID: 0000-0002-4401-3853)

PIRATA: A SUSTAINED OBSERVING SYSTEM FOR TROPICAL ATLANTIC CLIMATE RESEARCH AND FORECASTING

Bernard Bourlès[1], Moacyr Araujo[2], Michael J. McPhaden[3], Peter Brandt[4,5], Gregory R. Foltz[6], Rick Lumpkin[6], Hervé Giordani[7], Fabrice Hernandez[2,8], Nathalie Lefèvre[9], Paulo Nobre[10], Edmo Campos[11,12], Ramalingam Saravanan[13], Janice Trotte-Duhà[14], Marcus Dengler[4], Johannes Hahn[4], Rebecca Hummels[4], Joke F. Lübbecke[4,5], Mathieu Rouault[15], Leticia Cotrim[16], Adrienne Sutton[3], Markus Jochum[17] and Renellys C. Perez[6].

[1] IRD/Laboratoire d'Études en Géophysique et Océanographie Spatiales, Plouzané, France.
[2] Departmento de Oceanografia da Universidade Federal de Pernambuco – DOCEAN/UFPE, Recife, Brazil.
[3] NOAA/Pacific Marine Environmental Laboratory, Seattle, Washington, USA.
[4] GEOMAR Helmholtz Centre for Ocean Research Kiel, Germany.
[5] Christian-Albrechts-Universität zu Kiel, Kiel, Germany.
[6] NOAA/Atlantic Oceanographic and Meteorological Laboratory, Miami, Florida, USA.
[7] Météo-France/Centre National de Recherches Météorologiques, Toulouse, France.
[8] IRD/Laboratoire d'Études en Géophysique et Océanographie Spatiales, Toulouse, France.
[9] IRD/Laboratoire d'océanographie et du climat : expérimentations et approches numériques, Paris, France.
[10] INPE/Divisão de Modelagem e Desenvolvimento, São José dos Campos, Brazil.
[11] Oceanographic Institute, University of Sao Paulo, University of Sao Paulo, Brazil.
[12] Gulf Environments Research Institute, American University of Sharjah, United Arab Emirates.
[13] Texas A&M University, College Station, Texas, USA.
[14] Desenvolvimento Nuclear e Technológico da Marinha, Brazilia, Brazil.

This article has been accepted for publication and undergone full peer review but has not been through the copyediting, typesetting, pagination and proofreading process which may lead to differences between this version and the Version of Record. Please cite this article as doi: 10.1029/2018EA000428

[15] Nansen-Tutu Centre for Marine Environmental Research, DO/UCT, Cape Town, South Africa.
[16] Faculdade de Oceanografia da Universidade do Estado do Rio de Janeiro, FAOC/UERJ, Rio de Janeiro, Brazil.
[17] Niels Bohr Institute, Copenhagen, Denmark.

Corresponding author: Bernard Bourlès (bernard.bourles@ird.fr)

Key Points:

We describe the sustained tropical Atlantic observing system PIRATA maintained through a multi-national cooperative program in ocean science.

Major scientific results and accomplishments obtained from the last 10 years are presented.

The potential role of PIRATA in a future Tropical Atlantic Observing System is described.

Abstract:

PIRATA is a multinational program initiated in 1997 in the tropical Atlantic to improve our understanding and ability to predict ocean-atmosphere variability. PIRATA consists of a network of moored buoys providing meteorological and oceanographic data transmitted in real-time to address fundamental scientific questions as well as societal needs. The network is maintained through dedicated yearly cruises, which allow for extensive complementary shipboard measurements and provide platforms for deployment of other components of the Tropical Atlantic Observing System. This paper describes network enhancements, scientific accomplishments and successes obtained from the last 10 years of observations, as well as additional results enabled by cooperation with other national and international programs. Capacity building activities and the role of PIRATA in a future Tropical Atlantic Observing System that is presently being optimized are also described.

Plain Language Summary:

Long data records are essential for improving our understanding of the weather and climate, their variability and predictability, and how the climate may change in the future in response to anthropogenic greenhouse gas emissions. Climate variability in the tropical Atlantic Ocean has strong impacts on the coastal climate in particular and, consequently, the economies of the surrounding regions. Since 1997, the PIRATA program has maintained a network of moored buoys in the tropical Atlantic in order to provide instantaneous high quality data to research scientists and weather forecasters around the world. This paper describes PIRATA successes in terms of scientific discoveries and observing technology enhancements. Perspectives are also provided on PIRATA's role in the future Tropical Atlantic Observing System, currently under design, that will consist of a variety of coordinated measurements from satellites, ships, buoys, and other ocean technologies.

1 Introduction

PIRATA (Prediction and Research Moored Array in the Tropical Atlantic) is a multinational program initiated in 1997 to improve our knowledge and understanding of ocean-atmosphere variability in the tropical Atlantic, a region that strongly influences the hydro-climates and, consequently, the economies of the regions bordering the Atlantic Ocean (*e.g.* West Africa, Northern Brazil, the West Indies and the United States). PIRATA is motivated not only by fundamental scientific questions but also by societal needs for improved prediction of weather and climate variability and their impacts (Servain et al. 1998, Bourlès et al. 2008). PIRATA is maintained by a close collaboration between institutions in the USA (National Oceanic and Atmospheric Administration -NOAA), Brazil (Instituto Nacional de Pesquisas Espaciais -INPE, with contribution of the Diretoria de Hidrografia e Navegacão -DHN) and France (French Institut de Recherche pour le Développement -IRD and Meteo-France). These institutions established a formal partnership in 2001 through a Memorandum of Understanding to provide long term support for PIRATA. Other national observing initiatives in the tropical Atlantic have been closely cooperating with PIRATA activities including for example the German GEOMAR Tropical Atlantic Program, which allows for a coordinated development of the tropical Atlantic observing system.

.

PIRATA is based around an array of moored buoys providing meteorological and oceanographic data transmitted in real-time, disseminated via Global Telecommunication System (GTS) and Global Data Servers. Through yearly mooring servicing, data and sensors are calibrated and additionally high-frequency data recorded internally by the instruments are collected. The yearly cruises needed for the maintenance of the buoy array allow complementary measurements of a large set of physical, biogeochemical and biological data along repeated ship track lines and provide platforms for deployments of other components of the observing system. Several kinds of operations are carried out in collaboration with other national and international programs.

PIRATA is now more than 20 years old, well established and, after its international evaluation by the Climate and Ocean: Variability, Predictability and Change Program (CLIVAR) and the Ocean Observations Panel for Climate (OOPC) in 2006, has been recognized as the backbone of the tropical Atlantic observing system. PIRATA also serves as the baseline climate record in the tropical Atlantic through sustained observing of the Essential Climate and Ocean Variables (ECOV) defined by the Global Ocean Observing System (GOOS).

PIRATA provides invaluable data for numerous and varied applications, among which are analyses of climate variability on intraseasonal-to-decadal timescales, equatorial dynamics, mixed-layer temperature and salinity budgets, air-sea fluxes, model validation, data assimilation, and weather and climate forecasts. Real-time transmission data are routinely ingested in most operational weather and ocean centres worldwide.

The objectives of the present paper are first to describe PIRATA enhancements that have been achieved in recent years, including progressive updating of mooring systems and sensors; and second to present major scientific results of the core project as well as additional results obtained in cooperation with other national and international programs, which were made possible by PIRATA. Only results obtained from 2006 onwards are presented, *i.e.* after the 2006 PIRATA evaluation (Bourlès et al. 2008). A third objective of this paper is to demonstrate the use and impact of PIRATA data in climate research as well as in operational hindcast and forecast systems. Finally, we will describe the capacity building activities and perspectives of PIRATA as a central contributor to the Tropical Atlantic Observing System (TAOS) on the design of an enhanced and optimal network.

2 Evolution and present status of the PIRATA network

a) Ocean-atmosphere interaction buoys:

During the first years of PIRATA, when the program was named "Pilot Research Moored Array in the Tropical Atlantic", the program principally maintained an array of 10 meteorological and oceanic buoys in the tropical Atlantic (Servain et al. 1998). All buoys were ATLAS systems equipped with atmospheric sensors (air temperature, relative humidity, wind direction and amplitude, short wave radiation, rainfall) and oceanic sensors (11 temperature, 4 conductivity and 2 pressure sensors; see https://www.pmel.noaa.gov/gtmba/sensor-specifications for details). Daily averages were transmitted in real time through the Argos system and made available through the GTS, the PIRATA NOAA's Pacific Marine Environmental Laboratory (PMEL) website, and via anonymous ftp (https://www.pmel.noaa.gov/gtmba/pirata). After its evaluation by CLIVAR

and OOPC in 2006, the network progressively evolved, and the number of buoys increased to 17 in 2007, after extensions in the Southwest (3 buoys by Brazil) and the Northeast (4 buoys by the USA). PIRATA was subsequently renamed the "Prediction and Research Moored Array in the Tropical Atlantic" (Bourlès et al. 2008). An 18th buoy, funded by Benguela Current Large Marine Ecosystem in 2006, was deployed in the Southeast, off Congo, during a one-year test in 2006-2007; this location was re-established in 2013 with a 2nd buoy funded by the "Enhancing Prediction of Tropical Atlantic Climate and its Impacts" programme (PREFACE; https://preface.w.uib.no/) under the European Union's 7th Framework Programme (FP7).

The PIRATA network of meteo-oceanic buoys is part of the OceanSITES program (http://www.oceansites.org/OceanSITES/). In addition to the number of PIRATA buoys increasing since 2005, numerous additional sensors were progressively installed on a subset of the buoys, as summarized below:

- Since 2005-2006, 6 buoys have been equipped with additional sensors: 1 long wave radiation, 1 barometer pressure, 4 temperature and conductivity sensors along with 1 current meter at 12 m depth. These additional sensors allow for estimation of all components of the surface heat flux and improve the estimation of mixed layer depth. Thus, these buoys (namely at 15°N-38°W, 12°N-23°W, 0°N-23°W, 19°S-34°W, 10°S-10°W, 6°S-8°E) are referred as "Flux reference" sites.
- Since 2006 at 6°S-10°W and since 2008 at 8°N-38°W, CO_2 CARbon Interface Ocean Atmosphere (CARIOCA) sensors have been measuring the fugacity of CO_2 (fCO_2) at about 1 m depth, funded by the FP6 European project CARBOOCEAN (2005-2009).
- Beginning in 2008, dissolved oxygen (O_2) sensors were implemented at 4°N-23°W and 12°N-23°W at 300 m and 500 m to monitor the oxygen minimum zone (OMZ), funded by the German Collaborative Research Center 754 (SFB 754: "Climate-Biogeochemistry Interactions in the Tropical Ocean", 2008-2019) programme and the GEOMAR Helmholtz Centre for Ocean Research Kiel.
- Beginning in 2011, the buoy located at 20°N-38°W was equipped with a barometric pressure sensor, funded by Meteo-France.
- Beginning in 2011, additional temperature and conductivity sensors (with 9 temperature and conductivity sensors down to 100 m) were implemented at 6°S-10°W and 10°S-10°W, funded by IRD and the French Centre National de la Recherche Scientifique (CNRS).

Starting in 2015, the ATLAS systems have been progressively replaced by the more capable T-Flex systems, developed by PMEL (https://www.pmel.noaa.gov/gtmba/moorings). These buoys have a new modular design with off-the-shelf electronics and are able to provide more voluminous data transmission through Iridium instead of Argos.They allow the potential implementation of more sensors with high-frequency real-time data transmission. All ATLAS buoys will eventually be replaced by T-Flex, beginning with the "Flux reference sites". Three T-Flex systems were installed in late 2015 and early 2016 at 12°N-23°W, 0°N-23°W and 10°S-10°W. In March 2017, 4 T-Flex systems were also installed at 6°S-8°E (FR cruise), 4°N-23°W, 21°N-23°W and 20°N-38°W (USA cruise), and 3 T-Flex implemented in November-December 2017 at 0°N-35°W, 4°N-38°W and 15°N-38°W (BR cruise). Thus, at present there are 10 T-Flex systems operating in the array.

In March 2017, a new CO_2 CARIOCA sensor was implemented at 6°S-8°E, as an IRD contribution to the "Optimising and Enhancing the Integrated Atlantic Ocean Observing Systems" programme, funded by the European Horizon 2020 research and innovation project

(AtlantOS; https://www.atlantos-h2020.eu/). As a GEOMAR contribution to AtlantOS, the number of O_2 sensors was doubled by implementing three O_2 sensors with real-time data transmission at 21°N-23°W and 12°N-23°W. Internally recorded data is still collected with two O_2 sensors at 4°N-23°W, which is planned for implementation into the real-time data transmission in the future. The IRD contribution to AtlantOS also allowed the implementation of additional current meters at 10 m depth at three sites (8°N-38°W, 0°N-35°W and 0°N-10°W) and temperature/conductivity sensors at 5 m and 10 m depth at 0°N-10°W.

Also, the PIRATA buoys provide opportunities for other programs to maintain specific sensors, either as a contribution to long-term observations or as process-oriented studies. Beginning in 2014, i) all buoys have been equipped with acoustic receivers at 200 m depth, as a contribution to the Ocean Tracking Network (OTN; http://oceantrackingnetwork.org/), and ii) the 0°N-23°W and 0°N-10°W have been equipped with turbulence sensors (χpods), in the framework of an Oregon State University (OSU) Ocean Mixing Group program supported by the US National Science Foundation for a 5 years duration (http://mixing.coas.oregonstate.edu/). Also, in March 2017, 10 additional point acoustic current meters were implemented at 4°N-23°W between 7 m and 87 m depth for the NOAA/AOML "Tropical Atlantic Current Observations Study" (TACOS) experiment. This mooring was recovered in March 2018 and redeployed with 4 additional current meters between 27 m and 87 m to continue the TACOS observations of upper ocean velocity and its shear.

The present PIRATA network map is shown in Figure 1. Also shown are the different sensors added to the buoy network and the three adjacent Acoustic Doppler Current Profiler (ADCP) moorings (see below).

The overall delayed mode data return (for all moorings and all sensors; see Figure 2) is 81% over the entire period of the program (1997-2017), which exceeds the 80% data return standard used to gauge the success of the "Tropical Atmosphere Ocean" (TAO) array in the Pacific (McPhaden et al. 1998). Annual data return and number of moorings operating have been steady for several years and, since 2003, dedicated maintenance cruises have kept moorings within their design lifetime when they have been routinely performed.

The lowest values observed at the sites 0°N-10°W and 0°N-0°E are induced by vandalism associated with fishing activity in this area. However, vandalism has been considerably reduced during the past decade in the eastern part of the array: while from 1997 to 2007, these two buoys showed mooring survival values of 4.5/9 and 5/9 respectively, these values increased to 11/11 and 10/11 for the 2008-2017 period (see Figure 3) with the overall ratio for the PIRATA array being 145.5/149 (*i.e.* remarkably close to 1). In late 2017, the PIRATA mooring survival rate for the last decade was 100% for 13 sites (out of 18), which is an excellent overall result and a measure of PIRATA's success.

The annual PIRATA data return, in real time and delayed mode, varied between 67% and 91% from 1998 to 2016 and stabilized around 80% after 2003 (Figure 4). The last and exceptionally low value of 60% in 2017 (up to October 2017) is primarily due to vessel issues that resulted in a delay of several months to the Brazilian cruises carried out from November

2017 to January 2018. However, delayed mode data return values will become higher once data from the retrieved sensors are processed and made available.

PIRATA data files delivered through the web and ftp increased considerably after 2011, once files were made available through ftp (Figure 5). More than 600,000 files were retrieved in 2016 and 2017, illustrating the strong scientific and operational demand for PIRATA data.

b) Prototype ocean-atmosphere interaction buoy:

Also noteworthy is that in the early 2010's an effort was started to develop a Brazilian prototype of the ATLAS Buoy. This initiative was entirely sponsored by Brazilian agencies and conducted with technical support from NOAA/PMEL. In April of 2013, the first ATLAS buoy, entirely assembled in Brazil (the "ATLAS-B"), was successfully moored at 28°S-44°W, a position originally proposed for a fourth buoy of the PIRATA Southwestern extension (Cole et al. 2013, Campos et al. 2014). Presently the ATLAS-B is being prepared to be moored in the Vema Channel (31.13°S, 39.43°W). In this new position, the ATLAS-B will be equipped with sensors to monitor the northward flow of Antarctic Bottom Water, in addition to the regular monitoring of properties at the ocean surface and in the upper 500 m of the water column.

c) ADCP moorings:

PIRATA also maintains subsurface ADCP moorings (Figure 1) at 0°N-23°W (since 2001 with a gap in 2003) and 0°N-10°W (since 2006, initially as IRD contribution to AMMA/EGEE; Bourlès et al. 2007). These ADCPs typically allow monitoring the Equatorial Undercurrent from ~30 m depth down to about 300 m. For some periods, current meters at intermediate depths were also installed at 0°N-10°W (1999-2000 and 2003-2005) and at 0°N-23°W (2001-2002 and 2004-2006) in the framework of associated French and German programs (see, *e.g.*, Brandt et al. 2006; Bunge et al. 2008). Since 2006 the mooring at 0°N-23°W includes additional deep velocity measurements, partly from the surface to the bottom, that were carried out by GEOMAR contributions to different German projects. A new current meter mooring (also with an ADCP installed at 300 m depth looking upward) was deployed at 0°N-0°E in March 2016 during the PIRATA FR26 cruise. This mooring, deployed as an IRD contribution to the EU FP7 PREFACE program, will be maintained as part of PIRATA in the future. Each mooring is serviced every 1.5 to 2 years, and data are made available through the PIRATA-FR website (http://www.brest.ird.fr/pirata/) or through their DOI (http://doi.org/10.17882/51557).

d) Operations during annual servicing cruises:

PMEL surface moorings (ATLAS and T-Flex) have a design life of one year, thus requiring yearly cruises to maintain the array. These yearly cruises are carried out by Brazilian (western part), USA (north-eastern part) and France (eastern part) partners. The cruises provide a substantial number of shipboard measurements (mostly CTD casts along systematically repeated sections at 38°W, 23°W and 10°W and whenever possible including O_2 and LADCP velocity measurements), collect underway near-surface velocity and water mass property data, and contribute to several other programs (*e.g.*, by deploying Argo profilers and SVP drifters; radiosondes, ozonesondes, CTD and XBT data transmission in real time, aerosols, O_3, sea water analysis for nutrients, O_2, CO_2, Chlorophyll pigments, acoustic measurements…). All operations are summarized in Table 1, depending upon the country (see also Bourlès et al. 2017). Note that full-depth CTDO_2-LADCP casts were performed during the 2017 Brazilian cruise onboard R/V Vital de Oliveira, along with full-

depth bottle samples for salinity, O_2, pH and nutrients analysis, in addition to trace element analysis for GEOTRACES. At present, a total of 57 PIRATA dedicated cruises (28 by France, 17 by Brazil, 12 by USA) have been carried out in the tropical Atlantic, with repeated full sections along 38°W, 23°W (in addition to several cruises by GEOMAR made during the "Tropical Atlantic Climate Experiment" -TACE- and other German projects) and 10°W.

Most of the data sets acquired during the yearly cruise are made freely available through the national PIRATA websites, *i.e.* http://www.brest.ird.fr/pirata/ for the French cruises, http://www.aoml.noaa.gov/phod/pne/ for the USA cruises and http://pirata.ccst.inpe.br/en for the Brazilian cruises.

French CTD-O_2, vessel mounted ADCP and mooring ADCP data are also available through their DOI (http://doi.org/10.17882/51534, http://doi.org/10.17882/44635 and http://doi.org/10.17882/51557, respectively). The PIRATA-FR cruises and related information are also accessible through their DOI 10.18142/14. Moored and ship-based CO_2 data are available through the Surface Ocean CO_2 Atlas (SOCAT; www.socat.info).

Thanks to these yearly repeated cruises, PIRATA also significantly contributes to operational systems (*e.g.* MERCATOR and weather centers) by transmitting XBT and CTD profile data in near-real time and to the Atlantic Ocean Observing System in general (*e.g.* Argo, GDP/DBCP, etc.), as illustrated in Figure 6. Once off-line quality controlled, these T or T/S profiles are ingested in comprehensive historical dataset used worldwide in multi-decadal reanalyses (see section 5.3). As of January 2018, a total of 1683 CTD casts, 3861 XBT, 302 SVPs, 192 Argo profilers, 1007 radiosondes, and 194 ozonesondes have been deployed during the PIRATA cruises in the tropical Atlantic. The radiosondes and ozonesondes deployed during the US PIRATA cruises are done through a collaboration with the Aerosols and Ocean Science Expedition (AEROSE) group (Morris et al. 2006, Nalli et al. 2011).

3 Major scientific progresses since last review in 2006

3.1 Mixed layer heat and freshwater budgets

3.1.1 Equatorial heat budget

Sea surface temperature (SST) in the equatorial Atlantic experiences a strong seasonal cycle that interacts with the atmosphere to influence the seasonal variations in African monsoon circulation, rainfall, oceanic upwelling, and air-sea fluxes of heat and carbon. Superimposed on the strong seasonal cycle of SST are interannual variations that affect rainfall over South America and Africa and SST in the equatorial Pacific. Understanding the processes that drive equatorial Atlantic SST is therefore a high priority. Earlier studies identified the potential importance of upwelling and vertical turbulent mixing for generating seasonal cooling in the equatorial Atlantic during boreal spring and summer (Hastenrath 1977, Merle 1980, Molinari et al. 1985, Carton & Zhou 1997, Foltz et al. 2003, Peter et al. 2006). Over the past decade, this importance has been confirmed and progress has been made on identifying the processes responsible for the seasonal cycle of vertical turbulent mixing.

Observational studies of the equatorial mixed layer heat balance have concluded that vertical turbulent mixing drives seasonal cooling in the eastern Atlantic, consistent with modeling studies (Jouanno et al. 2011, Giordani and Caniaux 2011, Giordani et al. 2013, Planton et al 2018). Using measurements from the PIRATA mooring at 0º, 23ºW, Foltz et al.

(2013) showed a semiannual cycle in the heat budget residual, with largest negative values (*i.e.*, cooling from turbulent mixing) in May-July and November. This seasonality is consistent with that found by Jouanno et al. (2011) based on model experiments. In agreement with previous studies, Foltz et al. (2013) showed a close correspondence between vertical current shear below the mixed layer and vertical turbulent cooling of the mixed layer, with stronger shear linked to stronger cooling. The observational studies of Wade et al. (2011), Hummels et al. (2013, 2014) and Schlundt et al. (2014) further confirm the importance of vertical mixing for generating the Atlantic Cold Tongue (ACT) in the eastern Atlantic, with strongest cooling in boreal spring-summer. In addition to PIRATA data, some of these studies also used Argo profiles, shipboard CTD measurements and microstructure measurements (detailed in section 4.4). In the western half of the ACT (west of about 20ºW), there is agreement that zonal advection acts with turbulent mixing to cool SST (Jouanno et al. 2011, Giordani et al. 2013, Foltz et al. 2013, Hummels et al. 2014, Schlundt et al. 2014). However, the magnitude of the cooling is unclear because of difficulty quantifying zonal mixed layer currents.

An active field of research involves the processes that control turbulent mixing in the eastern equatorial Atlantic beyond large-scale seasonal changes in thermocline depth and vertical current shear. There is growing evidence that diurnal and intraseasonal variations of surface heat fluxes, winds, and currents are important for understanding the seasonal cycle. Hummels et al. (2013) showed a large increase in meridional currents and their vertical shear near the equator at 10ºW during the passage of a tropical instability wave (TIW) and suggested that TIWs may contribute substantially to shear variance during the second half of the year. Jouanno et al. (2013) showed that wind-forced Rossby-gravity waves, with periods of 8-10 days and 15-20 days, modulate thermocline depth and currents in the Gulf of Guinea (Figure 7). The increased shear associated with the waves drives vertical mixing, generating significant cooling of the sea surface. These waves are unrelated to TIWs located farther west.

There is also evidence that the diurnal cycle modulates turbulent mixing in the central equatorial Atlantic. Using PIRATA measurements at 0º, 23ºW and enhanced upper-ocean velocity measurements during October 2008 to June 2009, Wenegrat and McPhaden (2015) showed that there is strong seasonal modulation of the diurnal cycle of SST and vertical current shear in the upper ocean. During boreal summer and fall, trade winds are steady, and the diurnal cycle of SST is weak, resulting in weak stratification and the nighttime descent of a shear layer into the Equatorial Undercurrent (EUC). These conditions are favorable for generating deep cycle turbulence and enhanced cooling of the mixed layer. These findings are consistent with results obtained in the equatorial Pacific (Smyth et al. 2013, Pham et al. 2013, Moum et al. 2013), though the strength of diurnal mixing appears to be weaker in the Atlantic. Wenegrat et al. (2014) also showed using the 0°, 23°W data that the turbulent vertical viscosity depends fundamentally on the inverse of vertical current shear in the surface layer, a result heretofore not appreciated in simple parameterizations of turbulent viscosity in terms of the surface wind stress.

3.1.2 Off-equatorial heat budget

Outside of the equatorial band (2ºS-2ºN), there is evidence that cooling from vertical mixing is much weaker (Hummels et al. 2013, Foltz et al. 2013, Foltz et al. 2018). As a result, surface heat fluxes often play a more dominant role in shaping the seasonal cycle of SST (Foltz et al. 2013, Cintra et al. 2015). However, there remain significant seasonal variations in the heat budget residuals at some off-equatorial locations, implying that vertical

mixing and other processes may be important. Scannell and McPhaden (2018) for example inferred that at 6°S, 8°E on the southern margin of the ACT, upwelling and entrainment contributed to the seasonal decrease in SST during boreal summer. Foltz and McPhaden (2009) used PIRATA measurements to show significant seasonal variations of the heat budget residual at 12°N, 38°W and 15ºN, 38ºW. The largest residual cooling occurs in boreal summer and fall, when winds are weakest and solar radiation is strong. The explanation put forth from Foltz and McPhaden (2009) is that the salinity-induced barrier layer is thickest during boreal winter, suppressing vertical turbulent cooling of SST. During summer and fall the barrier layer is much thinner, promoting stronger turbulent mixing and SST cooling. However, Foltz et al. (2018) showed that the heat balance residual is consistently largest (*i.e.*, strongest implied vertical turbulent cooling) during the season with weakest winds and strongest diurnal SST variability, based on measurements from 17 PIRATA moorings. These results suggest that other processes, such as rectification of the diurnal cycle or enhanced current shear in a thinner mixed layer, may explain the seasonal cycle of turbulent cooling.

On interannual timescales, Rugg et al. (2016) used measurements from 12 PIRATA moorings, together with satellite data and ocean reanalysis output, to confirm that changes in latent heat loss and shortwave radiation are most important outside of the equatorial band. They also showed that anomalies of mixed layer depth, likely driven by anomalous winds, are an important component of the heat budget between 10ºS and 10ºN, where the mean mixed layer is thinnest. The thin mean mixed layer results in larger heat changes for a given wind anomaly, significantly altering the rate at which the climatological surface heat flux changes mixed layer temperature. Rugg et al. (2016) also confirmed an earlier study by Foltz et al. (2012) showing that anomalously strong vertical turbulent cooling was responsible for generating cold SST anomalies under the Intertropical Convergence Zone (ITCZ) during the boreal spring of 2009. The strong vertical turbulent cooling was caused by pronounced anomalous shoaling of the thermocline that was driven by anomalous northwesterly winds. The resultant SST anomalies generated a strong anomalous meridional SST gradient across the equator, which shifted the ITCZ southward and resulted in extreme flooding events in Northeast Brazil. Despite the importance of vertical cooling during 2009, Rugg et al. (2016) showed that there is inconsistency in the strength of the cooling from event to event. Nogueira Neto et al. (2018) have shown that the positive and negative SST anomalies observed in 2010 and 2012, respectively were the strongest in the last 30 years and were generated during the previous winter in both years, mainly north of 10°N, during which the wind anomalies were at the origin of intense latent heat loss anomalies. Horizontal advection also contributed to the maintaining of these SST anomalies in the equatorial zone and the south Atlantic.

3.1.3 Salinity budget

Strong precipitation and river runoff in the tropics lead to upper-ocean salinity stratification that tends to decrease the mixed layer depth, to enhance barrier-layer thickness and to reduce vertical mixing, while horizontal gradients of salinity contribute to the geostrophic circulation of the upper ocean (*e.g.* Kolodziejczyk et al. 2015). The continued successes of the Argo and PIRATA programs during the past decade, and the launch of two satellites (SMOS and Aquarius/SAC-D; *e.g.* Boutin et al. 2016) to measure Sea Surface Salinity (SSS) remotely, have contributed to significant advances in our understanding of the tropical Atlantic salinity budget during that period. Whereas earlier studies presented mainly large-scale and qualitative analyses due to limited *in situ* data, more recent efforts have started to quantify the processes involved in seasonal changes in SSS and their spatial variations.

One major difference between the mixed layer heat and salinity budgets is that for the salinity budget, horizontal advection is generally much more pronounced. This is due to multiple factors, including stronger spatial gradients of the surface freshwater flux due to strong precipitation in the ITCZ, strong freshwater input from rivers, and a lack of damping of SSS anomalies by the atmosphere as it occurs for SST anomalies. One region where advection is very important is the northwestern tropical Atlantic, where low salinity water is transported northwestward during the first half of the year (Foltz & McPhaden 2008, Coles et al. 2013, Da-Allada et al. 2013). In the central tropical North Atlantic, northward advection of low-salinity water from Amazon outflow and the ITCZ balances increasing tendencies in SSS due to evaporation and vertical mixing, resulting in a weak seasonal cycle of SSS (Foltz & McPhaden 2008, Camara et al. 2015). In the eastern tropical North Atlantic and under the mean position of the ITCZ, the seasonal cycle of precipitation is most important (Da-Allada et al. 2013). Grodsky et al. (2014) showed a local salinity maximum in the northwestern tropical Atlantic during boreal winter to early spring. This results from a minimum in Amazon discharge in fall, combined with transport of saltier equatorial and Southern Hemisphere water northward/westward, then eastward in the North Equatorial Counter Current (NECC). Therefore, in most regions of the tropical Atlantic, the mixed layer salinity budget represents a balance of multiple terms, including horizontal advection. On very large scales, for which advection becomes unimportant, Tzortzi et al. (2013) show that seasonal variations of precipitation and river runoff are most important.

Several recent studies investigated the mixed layer salinity budget in the equatorial Atlantic and Gulf of Guinea. In the Gulf of Guinea, river runoff and precipitation are compensated by vertical mixing and entrainment (Da-Allada et al. 2013). The net effect is an increase in SSS during May. Berger et al. (2014) came to a similar conclusion, showing that river runoff, vertical mixing, precipitation, and advection are important in the eastern Gulf of Guinea. Kolodziejczyk et al. (2014) and Da-Allada et al. (2017) showed that the boreal spring maximum in SSS in the ACT is explained by an increase in zonal shear and strong salinity stratification at the base of the mixed layer during December-May. Strong salinity stratification is due to ITCZ rainfall and freshwater advection from the east. Camara et al. (2015) also showed that strong vertical mixing in the eastern equatorial region balances freshwater advection. However, Schlundt et al. (2014) concluded that, during the onset of the ACT in the eastern equatorial Atlantic, horizontal advection and E-P are most important for the slight increase in SSS. Though important in the heat budget, vertical mixing was found not to be important for salinity budget due to strongly reduced salinity stratification after reaching maximum SSS in spring.

On interannual timescales, there is some evidence that changes in ocean circulation dominate in the western tropical Atlantic (Coles et al. 2013, Foltz et al. 2015, Fournier et al. 2017). However, there are also strong interannual variations in Amazon outflow that can contribute (Grodsky et al. 2014).

3.2 Equatorial circulation

One focus of the PIRATA observing system is the upper ocean circulation and its response to atmospheric forcing. Velocity measurements are taken by different current meters installed at the buoy systems or at the subsurface current meter and ADCP moorings nearby. Additionally, velocity data are taken by vessel mounted ADCPs used during PIRATA service cruises and by Global Drifter Program drifters and Argo floats deployed during these cruises. The acquired datasets have been strongly enhanced through cooperation with different

international and national projects such as TACE, 2006-2011 (Johns et al. 2014a) or the German Collaborative Research Center 754 (SFB 754) "Climate-Biogeochemistry Interactions in the Tropical Ocean", 2008-2019 (Brandt et al. 2015).

Subsurface moorings were deployed along the equator at 23°W (with almost continuous measurements starting in December 2001), at 10°W (since 2006), and at 0°E (from 2007 to 2011 during TACE and then since 2016 in the framework of PIRATA and PREFACE). Repeat velocity sections were taken and analyzed along 38°W in the tropical North Atlantic, along 23°W and 10°W across the equator as well as further east and closer to the African continent. Much attention was devoted to the variability of the EUC, which apart from the North Brazil Current is the strongest current in the tropical Atlantic. Previous studies (Johns et al. 2014b) suggested that the seasonal variability of the EUC in the central Atlantic cannot be explained by a quasi-stationary local momentum balance, because for example the near-surface velocity maximum of the EUC at 23°W in boreal spring occurs during the seasonal minimum of the easterly winds. Improved understanding of the seasonal cycle was gained by analyzing full-depth multi-year moored velocity measurements at the equator, 23°W allowing a decomposition of the seasonal cycle into the baroclinic mode-frequency space. This decomposition revealed distinct energy peaks located on the characteristic of resonant equatorial basin modes, which are defined by complete cycles of eastward and westward propagation of equatorial Kelvin and Rossby waves, respectively. The periods of such basin modes are a function of the phase speeds of the two wave types for the specific baroclinic mode and the basin widths. The importance of such resonance for the seasonal cycle in a realistic setting of the Atlantic Ocean was first shown for the second baroclinic mode semi-annual cycle by numerical modeling (Thierry et al. 2004). The full-depth mooring data could confirm the resonance behavior for the semi-annual cycle, but could additionally show a resonance for the fourth baroclinic mode annual cycle. The sum of the semi-annual and annual basin modes is able to explain largely the seasonal variability in the central equatorial Atlantic with an annual cycle in the EUC transport characterized by a maximum in boreal fall and a semi-annual cycle in the EUC core velocity, with velocity maxima in boreal spring and fall. The local timing of the seasonal velocity variability associated with the resonant basin mode cycle is not set by local wind forcing, but is a consequence of the integrated seasonal wind forcing in the inner tropics (Brandt et al. 2016).

In addition to the equatorial subsurface PIRATA moorings, moorings at 0.75°N and 0.75°S were deployed at 23°W, 10°W and at 0.75°S - 0°E during the TACE program (Johns et al. 2014b, Brandt et al. 2014). Together with the analysis of repeat ship sections (*e.g.* Hormann & Brandt 2007, Kolodziejczyk et al. 2009), the seasonal cycle of the EUC transport could be described along the equator. The seasonal cycle of the EUC transport varies along the equator featuring transport maxima at 23°W in boreal fall and at 0°E in boreal spring and a semiannual cycle in between at 10°W (Johns et al. 2014b). On interannual time scales, boreal summer EUC transport tends to be anomalously strong during cold Atlantic Niño events and weak during warm events (Brandt et al. 2014). Such behavior was associated by Richter et al. (2013) with so-called canonical events forced by zonal wind anomalies in the western equatorial Atlantic during boreal spring and associated Kelvin wave propagation. However, Richter et al. (2013) also identified non-canonical warm events forced instead by meridional advection from a warmer northern hemisphere toward the equator. For a specific non-canonical cold event in 2009, Burmeister et al. (2016) showed that meridional advection played only a minor role suggesting that this mechanism might be asymmetric regarding cold and warm events.

Within the PIRATA program, observations during yearly cruises in the otherwise not well sampled Gulf of Guinea were carried out regularly, which allowed a strongly improved description of the regional circulation and its variability and impacts. The termination of the EUC in the eastern equatorial Atlantic is characterized by a large variability in its position and strength, which is particularly reflected in the variability of the salinity distribution (Kolodziejczyk et al. 2014). The EUC generally transports high salinity waters eastward contributing via diapycnal mixing to the establishment of the seasonal SSS minimum along the equator one month before the onset of ACT in June (Da-Allada et al. 2017). At the termination of the EUC, high saline waters are mainly supplied to the westward currents north and south of the EUC, instead of being source waters for poleward eastern boundary currents (Figure 9). The strong weakening of the EUC at 10°W and 0°E during July and August (Johns et al. 2014b), together with enhanced mixing during the ACT season, interrupt the eastward salt transport, which is then reestablished in September with the strengthening of the EUC (Kolodziejczyk et al. 2014). Closer to the coast in the northern part of the Gulf of Guinea, the existence of the Guiana Undercurrent has been revealed. This eastward current, which is not directly supplied out of the North Equatorial Undercurrent, flows at subsurface north of the main path of the surface Guiana Current (Herbert et al. 2016). Further to the west at 23°W, the large number of shipboard velocity sections allowed the estimation of a robust mean flow characterized by an eastward surface flow between about 4°N and 9°N including the NECC and its northern branch (Urbano et al. 2006, Brandt et al. 2015). These eastward current bands were also identified along the 38°W PIRATA section (Urbano et al. 2008).

Superimposed on the energetic mean zonal current bands, there is weaker mean meridional flow associated with the shallow overturning in the tropical Atlantic. This is composed of the tropical cells confined to the upper 100 m between about 5°S and 5°N (Perez et al. 2014) and the subtropical cells connecting the equatorial upwelling with the subduction regions in the subtropics (Zhang et al. 2003, Schott et al. 2004). Preliminary results from the augmented point acoustic current meter data at 4°N, 23°W, find that the weak mean zonal and meridional currents at the surface are overwhelmed by meridional velocity fluctuations associated with TIWs that extend down to the depth of the thermocline (R. Perez, personal communication 2018). Foltz et al. (2015) showed, by incorporating PIRATA near-surface salinity data, the importance of the poleward surface flow of the northern subtropical cell for the meridional transfer of freshwater originating in the Amazon River discharge and rainfall below the ITCZ and resulting variability of SSS on seasonal and interannual time scales.

The equatorial Atlantic is characterized by strong intraseasonal variability that is well captured in upper ocean velocity data but similarly temperature and salinity measurements. Thus, PIRATA *in situ* measurements became extremely relevant in comparison to remote sensing data or for validating model results. Using satellite data, Athie and Marin (2008) could show that two types of intraseasonal waves dominate in the equatorial Atlantic: westward propagating TIWs dominate west of 10°W, and shorter period, wind-driven Yanai waves dominate in the Gulf of Guinea east of 10°W. Generally, intraseasonal variability has a great importance for the mixed layer heat budget (Hummels et al. 2013) due to the associated divergence in meridional and vertical heat fluxes, but at the same time intraseasonal waves provide energy to the deep ocean to maintain the equatorial Atlantic circulation (Ascani et al. 2015, Greatbatch et al. 2018), as presented in more detail in chapter 4.3. High-resolution model simulations that were validated against moored observation taken at the equator, 23°W were used to calculate eddy production rates and show that barotropic and baroclinic instabilities contribute to generate TIWs in the central equatorial Atlantic (Jochum et al.

2004, von Schuckmann et al. 2008), thereby confirming early results obtained from analyzing observational data (Grodsky et al. 2005). In general, the simulation of TIWs revealed a dependence of wave amplitude on the wind products used. By including short-term wind variability in the forcing, which is in agreement with direct wind measurements at the PIRATA buoys, Athie et al. (2009) were able to show that simulated TIW characteristics become more realistic with respect to the substantial interannual variability of TIW energy (Wu & Bowman 2007, Perez et al. 2012). TIW-related anomalies have also been studied using upper ocean temperature, salinity, and velocity data from PIRATA and current meter or ADCP moorings on the equator along 23°W (Grodsky et al. 2005, Wenegrat & McPhaden 2015). Besides the mixed layer temperature, mixed layer salinity was found to play an important role in TIW-related surface density anomalies, energy conversion associated with TIW-mean flow interaction, and its seasonality (Lee et al. 2014).

3.3 Ocean-Atmosphere-Land coupling and modes of variability

Interannual to decadal variability in the tropical Atlantic Ocean is typically described in terms of two climate modes: a meridional mode that is represented by an interhemispheric SST gradient, and a zonal or Atlantic Niño mode that is associated with SST variations in the eastern equatorial ACT region (*e.g.* Chang et al. 2006). The Atlantic Niño mode is similar to the El Niño-Southern Oscillation in the Pacific but more damped, mainly due to a weaker thermocline feedback (Lübbecke & McPhaden 2013). Pronounced SST anomalies also occur in the Gulf of Guinea and along the Southwestern African coast off Angola. The latter have been termed Benguela Niños (Shannon et al. 1986). Benguela Niños tend to occur before Atlantic Niños (Rouault et al. 2009, Lübbecke et al. 2010), and Lübbecke et al. (2010) suggest they are closely related.

These climate modes are of importance especially due to their impact on precipitation over the adjacent continents. Variations in rainfall over Northeast Brazil are closely related to SST variability in the tropical Atlantic Ocean (*e.g.* Hounsou-Gbo et al. 2015). In particular SST variability in the ACT is related to the West African Monsoon (Brandt et al. 2011a, Caniaux et al. 2011), and Benguela Niños have an impact on rainfall over southwestern Africa and coastal central Africa (Reason & Rouault 2006, Rouault et al. 2009, Lutz et al. 2015).

The coupled regional model study of Patricola et al. (2012) showed that deficiencies in simulated rainfall over the Amazon and Congo Basins can lead to biases in simulated SST in the equatorial Atlantic, and that air-sea feedbacks can amplify these biases. A coupled ocean-atmosphere study on the role of cloud cover parameterization on the rainfall distribution over the tropical Atlantic has suggested that the correct representation of deep atmospheric convection over the Amazon and Congo Basins are associated with the accurate representation of upper level atmospheric circulation pattern and the seasonal meridional migration of the Atlantic ITCZ (Bottino & Nobre, personal communication 2018). Giarolla et al. (2015) also documented that such improvements in continental atmospheric convection impacted positively the Atlantic EUC and the ACT.

Over the last decade, several studies have addressed the physical mechanisms of and the interaction between the tropical Atlantic climate modes. Measurements from the PIRATA array have been very valuable in many of these studies. PIRATA data have been used to investigate the processes at play in years of individual and composite meridional or Atlantic Niño events and to provide direct observation against which model output can be compared and validated (Foltz & McPhaden 2006a, 2008, 2009; Foltz et al. 2012; Rugg et al., 2016).

The PIRATA time series are now long enough to be used to investigate interannual variability.

The meridional and the Atlantic Niño modes have been dynamically linked through the reflection of Rossby into equatorial Kelvin waves (Foltz & McPhaden 2010b) and the discharge of off-equatorial heat content (Zhu et al. 2012). The connection between the meridional and Atlantic Niño modes also shows up in the warm water volume mode discussed by Hu et al. (2013). The meridional mode has also been linked to variability of the Guinea Dome in the northern tropical Atlantic (Doi et al. 2010). Atlantic Niños are further connected to Benguela Niños through the propagation of equatorial Kelvin waves with Benguela Niños actually leading Atlantic Niños by one to three months due to the different seasonal cycle of the thermocline depth in the two locations (Lübbecke et al. 2010). Benguela Niños are primarily forced remotely from the equator via equatorial Kelvin waves followed by poleward coastally trapped waves (Florenchie et al. 2003, Rouault et al. 2007, 2017, Imbol Koungue et al. 2017), even though local wind forcing might play a role as well (Richter et al. 2010, Bachèlery et al. 2016). This wave mechanism was also discussed from observations by Grodsky and Carton (2006). For the 2001 and 2011 Benguela Niño events, the associated equatorial Kelvin wave propagation can actually be detected in the PIRATA data (Rouault et al. 2007, 2017). Imbol-Kounge et al. (2017) show that all Benguela Niños are first detected as equatorial Kelvin waves by the PIRATA moorings along the equator one month before they start to appear off Angola (Figure 10).

There have been some specific warm and cold events that were investigated during the PIRATA period. One example is the anomalously cold 2005 ACT in the eastern equatorial Atlantic that has been related to an early onset of the ACT and strong intraseasonal wind bursts (Marin et al. 2009; Herbert & Bourlès, 2018). That event was also accompanied by exceptionally warm SST anomalies in the tropical North Atlantic, contributing to one of the most active and destructive hurricane seasons on record (Foltz & McPhaden 2006b).

Another dramatic event is the pronounced meridional mode event that took place in spring 2009, which has been explained by an anomalously strong high-pressure system in the subtropical North Atlantic and anomalous upwelling (Foltz et al. 2012). This event then led to a cold event in the eastern equatorial Atlantic in the following boreal summer through Rossby wave and reflected Kelvin wave propagation (Foltz & McPhaden 2010a, Burmeister et al. 2016). Atlantic Niños typically occur in boreal summer when the ACT is present, and the thermocline is shallow. Okumura and Xie (2006) found that there is also a secondary peak in the eastern equatorial Atlantic SST variability that occurs in November/December. They termed this mode Atlantic Niño 2. Although it has modest amplitude, it involves active interactions of zonal wind, upwelling, thermocline depth, and SST. It affects interannual fluctuations in rainfall in coastal Congo-Angola during the early rainy season and may also later affect precipitation in northeast Brazil in March-April. As shown by Grodsky et al. (2008) through ocean color products, these cold events also impact phytoplankton blooms.

PIRATA was also a key component of the international AMMA (African Monsoon Multidisciplinary Analysis) program, mostly through EGEE and associated cruises (2005-2007). Through *in situ* observations in addition to numerical simulations and satellite products, both programs allowed to show that: i) zonal wind anomalies in the western equatorial Atlantic during late boreal winter to early summer precondition boreal summer cold/warm events in the eastern equatorial Atlantic that manifest in a strong interannual ACT variability; ii) local intraseasonal wind fluctuations, linked to the St. Helena anticyclone,

contribute to the variability of ACT onset and strength, particularly during years with preconditioned shallow thermoclines; and iii) the impact of ACT SST anomalies on the wind field in the Gulf of Guinea is clearly demonstrated, and so contributes to the northward migration of humidity and convection and possibly the West African Monsoon jump (Hormann & Brandt 2007, 2009; Marin et al. 2009; Brandt et al. 2011a; De Coëtlogon et al. 2010; Caniaux et al. 2011).

Finally, a recent study by Awo et al. (2018) showed that both meridional and Atlantic Niño modes impact the SSS through atmospheric and/or oceanic processes. The atmospheric forcing, related to the ITCZ migration, controls the equatorial region, while advection due to modulation of circulation, vertical SSS gradient, and mixing at the base of the mixed layer drive SSS anomalies in the region under the influence of river plumes.

4 Additional results in cooperation with other national and international initiatives

4.1 Understanding CO_2 variability

The present day global ocean is a net annual sink of atmospheric CO_2 (Le Quéré et al. 2018). However, the tropical oceans are a CO_2 source to the atmosphere with large interannual variability controlled primarily by physical drivers (Padin et al. 2010). Sustained observing of surface ocean CO_2 in the tropics is critical for closing the global carbon budget (land, air, and ocean) and for understanding the fate of anthropogenic CO_2.

One of the objectives of the European CARBOOCEAN (2005-2009) project was to monitor CO_2 fugacity (fCO_2) in the Atlantic Ocean. A European network of CO_2 observations has been set up in which the CO_2 monitoring at the PIRATA sites was included. The sensors were built at the Technical Division of INSU (Institut National des Sciences de l'Univers) in France, and calibrated every year, before and after deployment. The first CO_2 sensor was installed in June 2006 at 6°S, 10°W, followed by the second one in March 2008 at 8°N, 38°W, during PIRATA-FR and BR cruises, respectively (Lefèvre et al. 2008), recording fCO_2, SST, and dissolved oxygen hourly in the surface ocean. The CO_2 network was further maintained during the European projects FP7 CARBOCHANGE (2011-2015) with additional support from IRD and INSU. These observations are part of the research infrastructure of ICOS (Integrated Carbon Observation System). A new CO_2 sensor has been installed on the T-Flex buoy at 6°S, 8°E in March 2017, funded by the European H2020 AtlantOS project. This buoy is located ~200 km off the Congo River mouth, aiming at better understanding the impact of large rivers on the CO_2 distribution in the tropical Atlantic.

The mooring at 6°S, 10°W is located south of the seasonal ACT and is affected by its migration from June to September (Lefèvre et al. 2008). It is also located above the mid-Atlantic ridge and subject to internal waves that increase surface fCO_2 and nutrients in the mixed layer (Parard et al. 2014). The region is a net source of CO_2 to the atmosphere (Parard et al. 2010). The net community production calculated from carbon and oxygen data averages 16.6 ± 6.1 mmol C $m^{-2}d^{-1}$ and exhibits a significant year-to-year variability (Lefèvre & Merlivat 2012). High frequency fCO_2 variability is observed throughout the time series but it is particularly pronounced after the upwelling season (Parard et al. 2010). The intraseasonal, seasonal and interannual variability of fCO_2 at this site has been explored by Lefèvre et al. (2016). On seasonal timescales, the fCO_2 variations are mainly correlated with SSS. At interannual timescales, some important differences appear in 2011-2012: lower fCO_2 and thus sea-air fluxes are observed from September to December 2011 and are explained by higher

advection of salty waters from the south to the mooring site, in agreement with the weaker zonal wind and a strenghtening of the meridional wind (Figure 11). In early 2012, the anomaly is still present and associated with lower SST. No significant long-term trend is detected over the period 2006-2013 on CO_2 or any other physical parameter. However, as atmospheric fCO_2 is increasing over time, the outgassing of CO_2 is reduced over the period 2006-2013 as the flux is mainly controlled by the difference of fCO_2 between the ocean and the atmosphere.

In the western tropical Atlantic, hourly measurements of fCO_2 and meteo-oceanographic data at 8°N-38°W site indicated two distinct seasonal periods (Bruto et al. 2017). During the first half year (January to July), the area is influenced by the North Equatorial Current with small salinity variations and the fCO_2 (mean fCO_2 378.9 µatm) is mainly controlled by SST changes. From August to December the air-sea CO_2 exchange (mean fCO_2 421.9 µatm) is associated with SSS variations induced by ITCZ rainfall and freshwater arrival from the Amazon River plume, which is transported eastward by the NECC after the retroflection of the North Brazil Current. Observed high-frequency (less than 24 hours) fCO_2 increases at 8ºN-38ºW are associated with rapid increases in SST resulting from diurnal cycle of solar radiation, combined with low wind speed periods that contributes to SST rising by inhibiting vertical mixing of colder waters. In contrast, observed high frequency fCO_2 decreases are associated with lower SSS values caused by heavy rainfall episodes.

The PIRATA cruises are also a good opportunity to collect additional data (such as seawater samples for inorganic carbon and alkalinity analyses) and to provide spatial information near the moorings. In 2006, underway fCO_2 was measured in the Gulf of Guinea during the French PIRATA cruise on board the R/V *Atalante*. A strong north-south CO_2 gradient was observed and associated with the two zonal currents (NECC-Guinea Current system and South Equatorial Current) with low fCO_2 measured in the warm and fresher waters north of ~2°N (Lefèvre 2009). During this cruise, the highest fCO_2 were measured in the coastal upwelling close to the Angola coast whereas biological activity explained a significant CO_2 drawdown near the Congo outflow. The seawater samples collected in the eastern tropical Atlantic since 2005 have confirmed the results and provided a robust alkalinity-salinity relationship for this region (Koffi et al. 2010), which allows the determination of all the inorganic carbon parameters at the 6°S, 10°W site. Similar work was done in the western tropical Atlantic with underway fCO_2 measurements made in 2009 and 2010 during the Brazilian PIRATA cruises on board the R/V Antares. The fCO_2 variability was mainly driven by physical processes and seasonal maps could be realized by developing empirical relationships (Lefèvre et al. 2014). Seawater samples collected for inorganic carbon and alkalinity as well as available data in this region led to new robust empirical relationships, as illustrated in Figure 12, and highlighted the role of the salinity in the variability of the carbon properties (Bonou et al. 2016). Such empirical relationships would allow to reconstruct the CO_2-system in the region for the full period of PIRATA deployment.

4.2 Oxygen minimum zone and equatorial ventilation

Oxygen minimum zones (OMZs) at intermediate depth (300 - 700 m) are present in the eastern basins of the tropical North and South Atlantic, representing the shadow zones of the ventilated thermocline in the tropical Atlantic (Luyten et al. 1983). They are separated by an equatorial oxygen maximum which is generated by energetic mean and variable zonal currents between 5°S and 5°N (Brandt et al. 2012).

In the past decade, repeat shipboard and moored observations taken within the German SFB754 in cooperation with the PIRATA program have significantly contributed to an improved understanding of the physical processes setting the mean state and the dynamics of the OMZ in the Eastern Tropical North Atlantic (ETNA; Karstensen et al. 2008, Fischer et al. 2013, Hahn et al. 2014, 2017; Brandt et al. 2015). The frequent repetition of the 23°W hydrographic section has revealed a dominant pattern of oxygen change in the ETNA between the years 2006 and 2015, characterized by a strong deoxygenation in the upper 400 m and a moderate oxygen increase between 400 and 1000 m (Figure 13). Changes in the large-scale circulation are considered as a major driver for the observed decadal oxygen change (Hahn et al. 2017). A larger scale multi-decadal oxygen decrease since the 1960s (Stramma et al. 2008, Brandt et al. 2015) was suggested to be driven by anthropogenic changes (Schmidtko et al. 2017), but natural variability of the climate system may play a comparable role (Frölicher et al. 2009, Keeling et al. 2010, Helm et al. 2011).

Moored oxygen observations from various latitudes in the ETNA have shown different regimes with oxygen variability on intraseasonal to interannual time scales. At the equator, interannual oxygen variability was observed to be associated with a 4.5-yr cycle of the equatorial deep jets (see next section 4.3) that contributes to a net eastward oxygen flux along the equator (Brandt et al. 2012). Intense mesoscale oxygen variability on intraseasonal time scales is present at the lateral boundaries of the OMZ resulting in a net meridional oxygen flux and being a major oxygen supply path toward the OMZ core (Hahn et al. 2014).

In recent years, the existence of extremely low-oxygen events in the ETNA has been revealed having severe impacts on local biogeochemical cycles and ecosystems. These so called dead-zone events, which occur at depths of about 50-300 m, are mostly associated with anticyclonic mode water eddies. They effectively transport water masses from the biologically productive eastern boundary upwelling system offshore into the open ocean. Strong oxygen reduction within eddies was found to be associated with an isolation of the eddy cores from its surroundings and enhanced consumption (Karstensen et al. 2015, Schütte et al. 2016).

In March 2017, oxygen time series at PIRATA buoys 12°N, 23°W and 21°N, 23°W were implemented into the online data stream of the T-Flex system for the first time. Providing real-time oxygen observations is a key element for the online monitoring of oxygen variability particularly including low-oxygen events.

4.3 Equatorial Deep Jets and possible climate impacts

PIRATA subsurface moorings typically deployed nearby the surface buoys are often used to install additional deep instrumentation. Along the equator deep velocity measurements partially covering the whole water column were carried out at 23°W starting in 2001 with a gap in 2003 and at 10°W from 1999 to 2005 with a gap in 2002/2003 (Bunge et al. 2008, Brandt et al. 2011b). Deep velocity data revealed a dominance of intraseasonal variability in the meridional velocity component, and strong semi-annual, annual and interannual variability of the zonal velocity component (Bunge et al. 2008). While the seasonal variability is generally associated with upward phase and corresponding downward energy propagation suggesting a dominant forcing at the ocean surface by the wind stress, the interannual variability was found to be associated with downward phase and upward energy propagation (Figure 14). The interannual variability has a distinct spectral peak at a period of about 4.5 years and is associated with relatively small vertical wavelengths of about 300 to 700 m corresponding roughly to the 16th baroclinic mode. It forms a system of vertically

stacked jets, the so-called Equatorial Deep Jets (EDJ). The EDJ are found to be responsible for the transport of tracers along the equator, like *e.g.*, CFCs (Gouriou et al. 2001) or oxygen (Brandt et al. 2008), and particularly contributes to the ventilation of the eastern equatorial Atlantic (Brandt et al. 2012). The upward energy propagation of the EDJ together with a statistical relation between the EDJ cycle and equatorial surface velocity, SST, wind stress and rain pattern suggest a climate impact of the EDJ (Brandt et al. 2011b). Due to the regular oscillations of the EDJ (because of their similarities with resonant equatorial basin modes), such an impact can improve climate predictions in the tropical Atlantic on interannual time scales. However, EDJ are typically not well simulated in realistic state-of-the-art ocean general circulation models (Ascani et al. 2015) because of their relatively low vertical resolution. Idealized simulations (Ascani et al. 2015) and the reconstruction of EDJ forcing derived from the 23°W mooring data (Claus et al. 2016) suggest an energy transfer from downward-propagating intraseasonal Yanai waves to the EDJ at intermediate depths. Using idealized simulations and velocity data from three moorings along 23°W between 0.75°N and 0.75°S, Greatbatch et al. (2018) showed that the meridional flux of zonal momentum associated with intraseasonal variability acts to maintain the EDJ against dissipation. The inclusion of EDJ or their effects in coupled climate simulations remains an open issue to be solved in the future.

4.4 Turbulent mixing from microstructure measurements

Extensive measurement programs using microstructure shear and temperature probes carried out in the 1980s and 1990s have greatly improved understanding of turbulent mixing processes in the upper thermocline of the tropical Pacific (*e.g.* Gregg et al. 1985, Moum & Caldwell 1985, Moum et al. 1989, 2009; Lien et al. 1995). However, prior to PIRATA, microstructure measurements had not been conducted in the open tropical Atlantic. During French PIRATA service cruises between 2005 and 2010 and other research cruises to the tropical Atlantic along 23°W and to the equatorial cold tongue, microstructure profiles were collected on a regularly basis prior to or following CTD stations. These data provided the first observational evidence for the variability of mixing processes in the tropical Atlantic and allowed quantification of vertical turbulent cooling of the mixed layer.

Hummels et al. (2013, 2014) determined vertical turbulent cooling of the mixed layer in the central and eastern equatorial Atlantic during May-December. This period encompasses the sharp drop in SST as the ACT is established during May-July and includes the following recovery of SST during August-December. The main result from these studies is that vertical turbulent cooling of the mixed layer is largest near the equator (2ºS-2ºN) and decreases significantly at off-equatorial locations. Mixing decreases eastward along the equator with values up to 50 W m^{-2} at 2ºE and not exceeding 10 W m^{-2} at 6ºE, confirming previous modeling studies (Jouanno et al. 2011, Giordani et al. 2013). Boreal summer was found to be the season with the highest rates of turbulent cooling throughout the equatorial ACT region, consistent with earlier estimates from the heat balance residual (Foltz et al. 2003). The analysis of the comprehensive set of observations revealed that the equatorially enhanced mixing rates are associated with the presence of strong vertically-sheared zonal flow induced by the eastward EUC and the seasonally-varying westward South Equatorial Current, forming a marginally stable environment for Kelvin-Helmholtz instability (Hummels et al. 2013, Wenegrat & McPhaden 2015). Seasonal and regional variability of diapycnal mixing within the ACT therefore varies in concert with the background conditions, namely vertical shear of horizontal velocities enhancing and stratification reducing mixing events and associated diapycnal fluxes (*e.g.* Hummels et al. 2013). Using PIRATA data and

microstructure data derived vertical cooling rates, Hummels et al. (2013) were able to close the seasonal mixed layer heat budget on the equator at 10ºW (Figure 15).

These findings compared well to mixing studies from the equatorial Pacific that had shown similar intense mixing at the equator (*e.g.* Gregg et al. 1985, Smyth et al. 2013). The main consequence of the equatorially enhanced turbulence below the mixing layer, both in the tropical Atlantic and Pacific, is the strongly enhanced diapycnal fluxes of heat, freshwater and nutrients that contribute to controlling the mean state and variability of SST, SSS and primary production (*e.g.* Gregg et al. 1985, Wang & McPhaden 1999, Moum et al. 2013, Hummels et al. 2013, Schlundt et al. 2014, Sandel et al. 2015). Furthermore, the results from the measurement program verified results from model studies that had shown elevated mixing to occur within the ACT region along with consequences for the heat and freshwater budget of the ACT and the Gulf of Guinea region (Jouanno et al. 2011, 2017; Da-Allada et al. 2013, 2014, 2017; Camara et al. 2015, Planton et al. 2018).

Starting in 2014, chipods measuring time series of the dissipation rate of thermal variance (Moum et al. 2013) were attached to the PIRATA moorings on the equator at 23°W and 10°W to monitor the variability of upper-ocean turbulent mixing processes.

4.5 Inertial Wave induced mixing

Recent studies carried out in the framework of the EU PREFACE programme focused on near inertial waves (NIWs), a process that is poorly resolved in climate models (Pillar et al., personal communication 2016, Bourlès 2016, Jochum 2017). Jochum et al. (2013) showed that NIW induced mixing brings cool subsurface water to the surface, and thereby modifies the tropical SST gradient and ITCZ position. The NIWs are principally generated by surface winds, with additional contributions from nonlinear interactions and other minor processes. Model-based estimates of the annual wind power input to the global surface ocean inertial frequencies span the range 0.3-1.4 TW, with significant uncertainty arising from sensitivity to the spatial and temporal resolution of the wind products employed and unresolved processes in the modeled ocean response. Thus, significant uncertainty surrounds the amount and fate of wind generated near-inertial energy in the ocean. Both observational and modeling studies have suggested that the majority of wind generated near-inertial energy is confined to the upper ocean, generating large shear across the mixed layer base. The resultant entrainment can lead to substantial deepening of the mixed layer following storms, with notable impacts on air-sea heat exchange and biogeochemical cycles. NIW strength is sensitive to details of atmospheric forcing, and there are only few observational constraints.

Long time series of continuous and concurrent high frequency surface wind (available at 6 of the 18 existing PIRATA moorings), and near-surface ocean velocity data are available to calculate the wind power input to near-inertial currents allowing exploration of the key characteristics of the inertial activity and wind power input to upper ocean near-inertial currents at each mooring (Pillar et al., personal communication 2016). As documented previously in mid-latitude studies (*i.e.* Dohan & Davis 2011), most of the near-inertial energy flux happens during clockwise rotating winds (early stage of hurricane Helene, September 2006; Figure 16). With the PIRATA array we have now an unmatched data set of co-located ocean surface velocity and winds that is being used to evaluate mixing parameterizations. It is troublesome, though, that the data is dominated by a few extreme events. While this allows us to test model performance on a case by case basis, it requires much longer time series to evaluate the long term mean effect of storm induced mixing (Figure 16). Time-mean near-inertial current speeds at the PIRATA moorings range from 3.6 cm s^{-1} to 13.0 cm s^{-1},

consistent with estimates from near-surface drifters. Analysis of these data provides new constraints on inertial energy injection and decay in the tropical ocean which are critical for refinement of existing near-inertial mixing parameterization, due to acute climate sensitivity to turbulence in the tropical mixed layer. The observed relation between near-inertial kinetic energy and mixed layer heat content, calls for better constraints on the vertical variation of upper ocean velocity, and highlights the value of furnishing the tropical moorings with additional current meters. In the long-term, a new parameterization scheme for the near-inertial mixing parameterization could be proposed that should improve significantly numerical simulations and predictions.

5 PIRATA data in ocean products and in operational analyses and forecasts

5.1 Product development and validation with PIRATA data

Since the last review of PIRATA in 2006, there have been over 60 papers published in the refereed literature using PIRATA data for satellite validation and for the generation, calibration, and validation of various satellite and/or *in situ* data products. The variables involved are SST (skin and bulk), SSS, surface wind speed and wind stress, specific humidity and air temperature, surface turbulent heat fluxes, short wave radiation, downwelling long wave radiation, precipitation, surface currents, and sea level. A full list of all the papers is contained in the PIRATA bibliography (regularly updated and accessible through http://www.aoml.noaa.gov/phod/pne/pdf/PIRATA_references.pdf). Here we highlight just a few studies to illustrate the broad application and utility of the PIRATA data.

PIRATA data have been incorporated into the surface marine meteorological "International Comprehensive Ocean-Atmosphere Data Set" (ICOADS) (Woodruff et al. 2011, Freeman et al. 2017). They have been used for assessing various SST products with high temporal (hourly to daily) resolution and spatial resolution (Kara & Barron 2007, Clayson & Weitlich 2007, Marullo et al. 2010, Reynolds & Chelton 2010). They have been used to validate Aquarius SSS measurements (Tang et al. 2014), to assess vertical variability of near-surface salinity in the tropics and the consequences of that variability for L-band radiometer calibration and validation (Henocq et al. 2010) and for assessing the temporal aliasing in satellite-based surface salinity measurements (Vinogradova & Ponte 2012). PIRATA data have been used in generating the OAFlux (Yu & Weller 2007) and Tropflux (Praveen Kumar et al. 2012) surface turbulent heat flux products and in the Tropflux wind stress product (Praveen Kumar et al. 2013). They were also incorporated into the Large and Yeager (2009) global climatology of interannually varying air-sea fluxes. The buoy data have been used to validate a high-resolution global ocean vector wind analysis constructed from passive radiometers and active scatterometers from 1987-present (Yu & Jin 2012) and in the evaluation of a variety of surface wind products (Peng et al. 2013). PIRATA data have been used extensively in studies to evaluate various tropical rainfall products (*e.g.*, Serra & McPhaden 2003, Bowman et al. 2009, Prakash et al. 2011, 2013; Xie et al. 2017) and surface radiation retrievals from satellites (Pinker et al. 2009, Wang & Pinker 2009).

PIRATA data have been incorporated into several climatologies based on *in situ* measurements, such as for SST and SSS. Reverdin et al. (2007) established monthly maps of SSS from a variety of sources including PIRATA moorings, between 30°S and 50°N, to study large-scale variability. They showed that seasonal SSS anomalies are found to respond with a 1-2 months lag to freshwater flux anomalies at the air-sea interface or to the horizontal Ekman advection. Similar products have been used in several studies related to SSS, *e.g.* Da

Allada et al. (2014b), who showed a SSS increase up to 0.5 over the period 2002–2009 in the Gulf of Guinea, off the Niger Delta.

As a contribution to Global Ocean Surface Underway Data initiative, members of the French CORIOLIS team established a process to systematically collect and validate (from sea surface water samples) the SST/SSS data acquired by all French Research vessel-mounted thermosalinographs during cruises and transits (Gaillard et al. 2015), including PIRATA-FR cruises. This "Sea Surface Salinity and Temperature from French REsearch Ships" (SSST-FRESH) dataset is very valuable for the calibration and validation of satellite observations delivered by the Soil Moisture and Ocean Salinity (SMOS) and Aquarius missions. In the same way, the In Situ Analysis System (ISAS) was established to produce gridded fields of temperature and salinity that preserve as much as possible the time and space sampling capabilities of the Argo network of profiling floats, using all types of vertical profile as well as time series, including PIRATA ones. ISAS gridded fields are entirely based on in-situ measurements. The system aims at monitoring the time evolution of ocean properties for climatological studies and allowing easy computation of climate indices. A careful delayed mode processing of the ISAS 2002-2015 dataset is made available through the French Sea scientific open data publication (Kolodziejczyk et al. 2017). ISAS has been used in several articles related to the tropical Atlantic to validate numerical simulations or as product for process studies (*e.g.* Da Allada et al. 2017, Jouanno et al. 2017).

Instrumental biases, data drop-outs, and the coarse vertical resolution of the oceanic measurements, sometimes complicate the use of PIRATA mooring data for research. An enhanced PIRATA data set (ePIRATA) was therefore developed for the 17 PIRATA moorings with record lengths of at least seven years (http://www.aoml.noaa.gov/phod/epirata/; Foltz et al. 2018). Data in ePIRATA are corrected for instrumental biases, temporal gaps are filled using supplementary data sets, and the subsurface temperature and salinity time series are mapped to a uniform 5-m vertical grid using information including Argo profiles. Important aspects of this data set are that all original PIRATA data that pass quality control and do not require bias correction are retained without modification, and detailed error estimates are provided for each daily-averaged oceanic and atmospheric parameter. The terms in the mixed layer heat and temperature budgets are calculated and provided, with error bars, as part of the ePIRATA data set. In addition to its value for upper-ocean and climate research and model validation, ePIRATA presents a framework for assessing the value of additional PIRATA sensors for reducing uncertainties in upper-ocean temperature and salinity, mixed layer depth and currents, and mixed layer heat and temperature budget components.

To address the relevance of thermistor chains on free-drifting buoys and evaluate the potential future use of such material equipped with other physico-chemical parameters (such as salinity or dissolved oxygen) an analysis has been carried out in the framework of the EU AtlantOS program to revisit data collected by such equipment, some deployed in 2006 and 2015 during PIRATA cruises in the Gulf of Guinea (Rousselot et al. 2017). The analysis is based upon the co-localization of nearby buoys, thermosalinograph data, Argo data, PIRATA buoy data, and CTD profiles. A new model must be applied to settle the sensors to fixed depths when the bottom of the chain is lifted up, resulting in biases that usually do not exceed 0.2°C. The reduced level of accuracy renders this kind of instruments a useful tool for surface ocean observation. Thus, corrected data sets have been provided to the CORIOLIS "Global Data Assembly Centre" (GDAC).

Yearly PIRATA cruises may be opportunities for some specific operations. The PIRATA-FR15/EGEE-3 cruise carried out in May-July 2006 allowed documenting the ocean-atmosphere system with high frequency meteorological measurements and 251 radiosoundings (Bourlès et al. 2007). Such data sets, also used in combination with modelling experiments and "European Centre for Medium-Range Weather Forecasts" (ECMWF) analyses, allowed to investigate the links between SST and the marine atmospheric boundary layer in the Gulf of Guinea, and the air–sea interaction impact on the water cycle (*e.g.* Leduc-Leballeur et al. 2011). They also allowed to test cumulus, microphysics and radiative parametrizations used in the Weather Research and Forecasting (WRF) model, showing that such parameters exert a large influence on the simulated seasonal distribution of regional convective rainfall (Meynadier et al. 2015). Turbulent fluxes at the air-sea interface were also estimated from flux measurements obtained from a dedicated mast installed on the R/V *Atalante* during this particular cruise. Turbulent fluxes were calculated with an eddy covariance method and with a spectral method. Calculation of eddy correlation fluxes required a correction of flow distortion at turbulent scales, which was performed with a new statistical technique. Application of the spectral flux calculation method revealed that an imbalance term was required, in agreement with results from earlier experiments, and indicated that the value of the Kolmogorov constant (0.55) should not be modified. Bulk exchange coefficients calculated are in good agreement with earlier parameterizations in medium wind conditions (Bourras et al 2009). Turbulent fluxes at the air-sea interface were also estimated from flux measurements obtained from a micrometeorological tower installed on the R/V *Vital de Oliveira* during the PIRATA-BR XVII cruise during October 2017-January 2018.

Radio-soundings and oceanic data from oceanographic campaigns in 2006 (EGEE-3/PIRATA-FR15) and 2014 (PIRATA-FR24), airborne measurements in 2016 (DACCIWA campaign), *in situ* data from PIRATA buoys, and high-frequency satellite data (as "Météosat Seconde Génération" classifications in 2008, 2012 and 2014, "Advanced Microwave Sounding Unit" data or "Tropical Rainfall Measuring Mission" -TRMM- precipitation), in addition to coupled regional simulations (WRF-NEMO) and reanalyses (ECMWF ERA-I and "National Centers for Environmental Prediction" -NCEP- "Climate Forecast System Reanalysis" -CFSR-), have also been used to study the atmospheric response to the diurnal cycle in the Gulf of Guinea. The diurnal cycle of deep convection (and its change of phase, from a midday oceanic convection to a late afternoon continental convection), as well as its dynamical conditions in the low-level atmosphere, could be regionally mapped (Bourlès, 2016). The question investigated is which frequency of ocean-atmosphere exchanged is required in a coupled regional model in order to correctly represent the diurnal cycle and seasonal evolution in the northeastern tropical Atlantic in boreal spring and summer (when the seasonal onset of cold equatorial upwelling intensifies the air-sea interaction), and which vertical resolution is needed in the lower atmosphere.

The NCEP reanalysis and reanalysis from the CFSR (Saha et al. 2010) product allowed, as a typical example, a study based on satellite observations and WRF simulations forced by different SST patterns, to analyze the role of the air-sea interaction in the Gulf of Guinea in setting precipitation at the Guinean coast during the onset of the West African Monsoon (Meynadier et al. 2016). This study clearly showed that the seasonal ACT setup strongly constrains the low level atmospheric dynamics between the equator and the Guinean coast. The local SST meridional gradient has noticeable effects on the marine boundary layer stability and hydrostatically-changed meridional pressure gradient, which strongly impacts moisture flux convergence near the coast. It particularly showed that the SST influences the

wind through a local modification of the pressure gradient (Lindzen and Nigam's mechanism). The fast adjustment of the vertical stratification in the mixed-layer is also significant in the equatorial area after the ACT onset, but not before, emphasizing a threshold effect.

The water vapour in the lower atmosphere is a key component of earth's climate system. It is expected that the recent warming of the earth surface will strongly influence sea surface evaporation and precipitation patterns. The PIRATA-FR24 cruise provided an opportunity to measure water vapour isotopic composition ($^{1}H_2{}^{16}O$, $H_2{}^{18}O$ and $^{1}H^{2}H^{16}O$) of the Atlantic marine boundary layer, by using Picarro and weather station measurements. The most enriched water vapour isotope values, signature of evaporation processes, were observed during periods dominated by the trade wind regime with limited atmospheric convection. The most depleted isotopic values, signature of dilution processes, were recorded during periods of strong convective activity in the Gulf of Guinea. These data sets also allowed demonstrating the impact of tropical upwellings and mesoscale SSS patterns on water vapour composition, suggesting that high-resolution isotope sampling can identify advection processes, even if salinity variations are small (Benetti et al. 2017a, 2017b).

Recently, Trolliet et al. (2018) carried out a study using PIRATA buoy solar irradiance measurements for satellite product validation, as a continuation of the study by Boilley and Wald (2015). The data sets comprise the re-analyses MERRA-2 and ERA-5 and three satellite-derived data sets: HelioClim-3v5, SARAH-2 and CAMS Radiation Service v2, and are compared to qualified measurements of hourly irradiance made at five buoys of the PIRATA network for the period 2012-2013. The re-analyses often report cloud-free conditions while actual conditions are cloudy and reciprocally, actual cloudless conditions as cloudy. The medium and high-level clouds exhibit more bias than the low-level clouds. The re-analyses poorly correlate with the optical state of the atmosphere derived from the measurements. The actual irradiance field is spatially distorted by re-analyses, especially for MERRA-2. Performances are similar between the three satellite-derived data sets. They correlate well with the optical state of the atmosphere and reproduce well the dynamics of the solar irradiance. The three data sets exhibit overestimation with the lowest biases reached by CAMS Radiation Service v2. The bias of HelioClim-3v5 is fairly similar from one location to the other, which means that the actual spatial gradients are well reproduced. This study revealed that PIRATA network is a unique and valuable means to study and monitor the surface irradiance in the tropical Atlantic Ocean and deserves support for operations to further enrich the data records.

5.2 PIRATA data use for numerical model validation

PIRATA buoy and cruise data are used extensively for model validation. Most of the results summarized above (equatorial circulation, mixed layer processes, TIWs, deep jets, etc.) are based on numerical models validated with *in situ* and other measurements including PIRATA data (*e.g*. Hormann & Brandt 2007, von Schuckmann et al. 2008, Silva et al. 2009, Kolodziejczyk et al. 2009, 2014; Jouanno et al. 2011, 2013; Cintra et al. 2015, Brandt et al. 2016, Imbol Kongue et al. 2017). One other example was the shipboard ADCP data from the Brazilian maintenance cruises for the period 1998-2005, which were used to validate previous numerical simulations that predicted the existence of the northern branch of the NECC (Urbano et al. 2006, 2008). Also, PIRATA ADCP data were used to validate ocean and coupled ocean-atmosphere modeling of the Atlantic EUC by Giarolla et al (2005, 2015). In Giarolla et al. (2015), the Brazilian Earth System Model - BESM-OA2.5 representation of both the phase and amplitude of the equatorial ACT is contrasted with those of other CMIP5

models. The thermally indirect nature of the South Atlantic Convergence Zone has been demonstrated by the use of both PIRATA data (temperature, rainfall, and solar radiation; see Table 2) and coupled ocean-atmosphere simulations with the BESM-OA2.3 model (Nobre et al. 2012). Similarly, PIRATA data were used to validate numerical simulations which show that the observed increase in Agulhas Leakage might be correlated with changes in thermodynamic properties and ocean-atmosphere fluxes in the western Tropical Atlantic (Castellanos et al. 2016, 2017). Additionally, PIRATA data have been used for validation in model studies to identify the origin of warm SST biases in the eastern tropical Atlantic exhibited by coupled general circulation models. Xu et al. (2014) analyzed mechanistic regional ocean model simulations, PIRATA mooring measurements and reanalyses to link the warm SST biases in the southeast Tropical Atlantic to subsurface bias in the equatorial thermocline.

Recently, hydrographic and acoustic measurements obtained during the French PIRATA cruise from 2015 onboard the R/V *Thalassa* were used in a numerical model dedicated to investigating spatiotemporal dynamics of fish populations under the influence of both fishing and environment, the "Spatial Ecosystem And POpulation DYnamic Model" (SEAPODYM; *e.g.*, Lehodey et al. 2015; see also www.seapodym.org). Observing System Simulation Experiments (OSSE) were carried out with the SEAPODYM Mid-Trophic Level (MTL) component to analyze the biomass distribution of micronekton in the Eastern tropical Atlantic and to assess the benefit of using different observation networks in data assimilation procedures. Such experiments clearly demonstrated that, due to its localisation and its sampling scheme during cruises, the PIRATA network is one of the best observation networks for data assimilation in SEAPODYM-MTL (Delpech et al., personal communication 2017), proving that PIRATA may also be relevant for biological research.

5.3 PIRATA data use in operational meteorology and oceanography

Operational oceanography is now well established in many countries with the aim to provide reliable ocean products devoted to describe and predict marine environment status and dynamics for a wide range of users and policy makers (Schiller et al. 2016). Depending on their socio-economic interest, countries are developing regional, global forecasting systems, or both. First these systems were designed to describe the physical ocean dynamics, including sea ice, based on ocean model corrected on weekly or daily basis by assimilation (Tonani et al. 2015), with forecast length of 3 to 15 days. Then, some of these systems incorporated coupling with the biogeochemical modelling, to provide low trophic level description, carbon and oxygen content variability (Gehlen et al. 2015), and as a byproduct pH variation, to support the global change monitoring (Gehlen et al. 2011). In the very recent years, coupling with atmospheric or wave models has also been commenced, in order to better represent the correct fluxes between ocean and atmosphere for short term forecast (Brassington et al. 2015).

The operational systems of Mercator Océan are based on the NEMO/PISCES ocean models and a Kalman filter that assimilates the PIRATA data (Lellouche et al. 2013). Temperature and salinity profiles are assimilated on a daily basis. Note that Mercator Océan systems are forced by ECMWF atmospheric fluxes that are also using PIRATA measurements (meteorological and surface ocean temperature).

Real time forecasting global systems offer now eddy-permitting to eddy resolving capabilities, assimilating satellite altimetry and radiometry derived information, and in-situ temperature and salinity observations. Most of the time, these systems assimilate the

available vertical profiles from Argo, XBT lines, CTD from oceanographic cruises, and data from mooring, including the TAO-PIRATA-RAMA ("Research Moored Array for African-Asian-Australian Monsoon Analysis and Prediction") arrays. Timeliness is the main limitation for many operational systems that might have assimilation window of few hours (*e.g.*, Blockley et al. 2014). PIRATA temperature and salinity mooring data are transmitted in quasi-real time to the GTS and to some GDACs, and most global operational systems are assimilating them. The transition from Argo (ATLAS buoys) to Iridium (T-Flex buoys) satellite transmitting systems has significantly improved data timeliness. The direct impact of PIRATA data on real time hindcast has been evaluated positively several times (Lea et al. 2014, Oke et al. 2015, Poli 2018).

Operational ocean centers and meteorological centers that carry out short to medium terms predictions (seasonal to interannual forecast) through forced or coupled ocean-atmosphere systems are also producers of global ocean reanalyses, as Ocean ReAnalysis Pilot 5 from an eddy-permitting ocean (Zuo et al. 2017), and air-sea heat fluxes (Valdivieso et al. 2017). Evaluation of these global ocean reanalyses, providing eddy-permitting and intra-seasonal scale variability description (*e.g.*, Masina et al. 2015) needs all available data to be assessed, and in particular the multiparametric data set provided by the PIRATA effort since 1997. At the surface, Liu et al. (2017) proposed an evaluation of satellite and reanalysis-based global net surface energy flux and uncertainties. During the recent ocean reanalyses intercomparison project under the auspices of CLIVAR/GSOP and GODAE OceanView, most of the global eddy permitting reanalyses over the past 20 years were assimilating PIRATA data (Balmaseda et al. 2015) using the qualified dataset CORA (Cabanes et al. 2013) or EN4 (Good et al. 2013). One of the obvious benefits of the PIRATA array has been to provide, since 1998, temperature and salinity profiles in the Tropical Atlantic where Argo floats were not providing significant information before 2002. Ocean reanalyses and operational hindcasts are also used to provide in near real time an assessment of the ocean climate changes. For instance, every month, the tropical oceans evolution is analysed through a series of ocean indicators (*e.g.*, Xue et al. 2017). An annual assessment mostly based on ocean reanalyses is also performed by the European Copernicus Marine Service (von Schuckmann et al. 2016).

The *in situ* temperature and salinity profiles that are available in real-time are also used for validation by operational centers, even if assimilated or not. In the frame of GODAE OceanView, and also as part of the Copernicus Marine Environment Monitoring Service, dedicated working groups have been designing these past years' real-time assessment methods based on the existing available dataset. In particular, the Class-4 metrics approaches where temperature and salinity forecast are compared to observations in order to determine skill scores and the performances of operational systems in real-time (Hernandez et al. 2015).

6 Capacity development

PIRATA has efficiently contributed to capacity building in developing countries bordering the tropical Atlantic. As an example, a regional Master's Degree program dedicated to Physical Oceanography and Applications was initiated in 2008 in Benin, West Africa, thanks to a collaboration between IRD, University Paul Sabatier of Toulouse and the UNESCO International Chair in Mathematical Physics and Applications (ICMPA) of the University of Abomey-Calavi in Benin (Danuor et al. 2011), also with the support of the French oil company Total from 2009 to 2015. Graduates of this Master's Degree program

include about 30 doctoral students who have subsequently occupied positions on both sides of the Atlantic (Benin, Ivory Coast, Cameroon, Senegal, South Africa, France, Germany, Brazil and Canada). This Master's program is currently evolving into an international cooperation between Benin, France and Brazil, continuing to reinforce north-south links and developing south-south partnerships, as envisioned with the "Belem Statement" (see https://www.atlanticresource.org/aora/belem-statement).

PIRATA cruises also represent an opportunity for students and young scientists to receive training in measurements at sea. For example, more than 60 African and Brazilian young scientists/students have been trained during French and Brazilian cruises since 2000. Similarly, USA cruises, through collaborations with projects like AEROSE, provided the basis for student education with over 55 students being trained in shipboard measurements (over 70% of students from under represented groups) during the last 12 years.

Several summer schools were organized, some linked to the EU PREFACE program, during which several African students could benefit from training on tropical Atlantic issues or using PIRATA data. Up to 44 students and young scientists, mostly from Brazil and West Africa, attended the last summer school organized during the annual PIRATA meeting held in November 2017 at Fortaleza, Brazil.

These past years, PIRATA annual meetings have been organized jointly with other initiatives raising scientific discussion about the Tropical Atlantic (TACE, PREFACE, AtlantOS...), allowing more comprehensive events, where a larger audience was discussing more multidisciplinary issues. Such events allowed to enhance the scientific community, in facilitating serendipity and emerging collaborations. They also welcomed new generations of scientists from Europe, Africa, North and South America.

7 PIRATA in the future

First and foremost, it is essential to continue the long time series at the mooring sites that have already been established. The records at these sites are now long enough to study not only intraseasonal to interannual time scale variability, which were the original targets of the array, but now also interannual to decadal variability and climate change. The value of these time series will increase with time as the records get longer, to reveal how natural variability across a wide spectrum of time scales in the tropical Atlantic is affected by a changing background state (*e.g.* Servain et al. 2014) and how variability and trends affect the climate system.

Beyond sustaining the moored time series at sites that have been producing invaluable data for the past two decades, we see several enhancements to the existing array. These include: 1) adding more instrumentation in the near surface layer to better define mixed layer structures, processes, and ocean-atmosphere feedbacks; 2) multi-disciplinary enhancements for carbon cycle and biogeochemical studies; and 3) expanding the array into regions that are presently undersampled (or unsampled) by moored time series and that would benefit from high temporal resolution, multi-variate, and multi-disciplinary sustained time series.

Observational programs already underway in the tropical Atlantic will help to address some of these goals. These include moored microstructure measurements from equatorial PIRATA moorings, additional salinity sensors on PIRATA moorings in the western tropical

Atlantic, and the TACOS process study involving deployment of multiple current meters in the upper 100 m on the 4ºN, 23ºW PIRATA mooring. However, additional sustained measurements of salinity, temperature, and velocity in the upper 100 m at selected locations will be needed for a comprehensive analysis of the mixed layer heat budget on diurnal to intraseasonal timescales. Also, additional salinity and velocity measurements in the upper 100m on PIRATA moorings will likely be most beneficial for closing the salinity budget, as for example at 6°S, 8°E where the Congo River outflow induces strong vertical stratification with impacts on local and regional circulation, mixing, and SST. Enhanced sensor suites are now possible on T-Flex systems that allow in addition high-frequency real-time data transmission. In the near term, all PIRATA buoy sites will be equipped with T-Flex systems.

The need for biogeochemical measurements is crucial for addressing several issues related to the global carbon cycle, nutrient balances, ocean deoxygenation, living marine resources, and ecosystem dynamics (*e.g.* Hernandez et al. 2017). Biogeochemical low trophic levels and carbon dynamics are also in the scope of operational oceanography that implements coupled prediction systems assimilating satellite chlorophyll data (Gehlen et al. 2015). Their improvements depend on calibration and verification supported by carbon, oxygen and nutrient measurements. Some PIRATA buoys are already equipped with CO_2 and O_2 sensors and need to be maintained on the long-term. More of these and other biogeochemical sensors would be very valuable as well. For example, although the western tropical/equatorial Atlantic does not exhibit an oxygen minimum zone like in the eastern tropical Atlantic (Brandt et al. 2015), PIRATA cruises' measurements (Urbano et al. 2008) and Argo float O_2 data from 2015 (Cotrim, personal communication) indicate that one may find lower oxygen concentrations at intermediate depths. Although the intermediate water is not hypoxic, oxygen saturation levels reach 20%. What establishes these features? Are they related to the highly productive Amazon plume and/or to the current system? Urbano et al. (2008) have also proposed using O_2 as a water mass tracer along the western tropical Atlantic, using PIRATA cruise data. Also, in contrast to the ETNA region, very little O_2 data exist to investigate the OMZ variability in the eastern tropical South Atlantic. Further long-term O_2 measurements in the western and southeastern PIRATA array could be envisioned to address these issues.

Likewise, enhancing ocean surface pCO_2 measurements on the PIRATA buoys would improve the knowledge of tropical Atlantic air-sea CO_2 fluxes, the region's CO_2 flux influence on the global carbon budget, and the behaviour of ocean biogeochemistry under increasing levels of atmospheric CO_2. More CO_2 measurements, particularly in the western and central parts of the PIRATA array, will link the programme to the international SOLAS project (www.solas-int.org), to the regional (and primarily coastal) initiatives on ocean acidification (OA) studies. These studies include BrOA - Brazilian OA network (www.broa.furg.br), and LAOCA - Latin American OA network (www.laoca.cl), and the global initiatives, GOA-ON and SOCAT. Also, in order to document surface OA trends, it is necessary to monitor at least two measurable parameters of the marine CO_2-system, *i.e.* some combination of fCO_2/pCO_2, total CO_2 (TCO_2; a.k.a. dissolved inorganic carbon [DIC]), pH, and total alkalinity (AT). At present, there are available commercially autonomous sensors for fCO_2/pCO_2 and pH that are already used in combination by NOAA through their Ocean Acidification buoys, *e.g*. the RAMA Bay of Bengal Ocean Acidification (BOBOA) mooring. Similar capabilities, including bottle measurements during cruises, should be included in the future. .

Geographical extension of the PIRATA buoy network can also be envisioned, through either new resource commitments by the partners and/or through the involvement of other partners and countries. In particular, observations are crucially needed in the South Atlantic where no time series and relatively few historical *in situ* measurements are available, particularly in the southeastern part of the basin (*e.g.* Zuidema et al. 2016). For example, new time series measurements would be especially valuable to accurately determine air-sea fluxes in the Saint-Helene anticyclone and to validate analysis/re-analysis products used for research and forecast model initialization (Herbert & Bourlès, 2018). The northwestern part of the basin, *i.e.* the tropical Atlantic warm pool, is under the influence of the runff of Amazon and Orinoco rivers creating strong upper-ocean salinity stratification. Additional buoys are here required to better assess the mixed-layer heat budget (*e.g.* Nogueira Neto et al. 2018) and the impact of fronts and eddies on air-sea fluxes and mixing. Such buoys would also allow for better monitoring of tropical cyclones' and hurricanes' westward evolution.

So, the future tropical Atlantic buoys network could be envisioned as in Figure 17:

Sensor enhancements on existing buoys could be ensured through additional collaborations and funding. On the other hand, potential extensions of the mooring network, *e.g.* through additional PIRATA buoys, will require ship time above and beyond that already being provided by the present PIRATA partners (USA, France, Brazil). Where precisely that ship time might come from is an open question, though it is likely that a South Atlantic extension would require cooperation between South Atlantic bordering countries (South Africa, Brazil, Argentina, Namibia, Angola…) that have both the necessary vessel and technical capacity.

Thus, the availability of ship time, which is the most expensive component of observing systems, on research vessels capable of deep sea mooring operation to service the array, is critical. Flexibility among ship operators to work together to ensure adequate ship time is essential to ensure the yearly mooring/repeat hydrography operations. Managing ship time for the core mooring and associated activities is an ongoing major challenge.

Servicing a monitoring network in the long term requires some commitments between institutions in charge of its maintenance. PIRATA in its 21st year is a good example of ongoing success, made possible thanks to a stable base of support in the three involved countries and commitments of each country's involved institutions through a Memorandum of Understanding. Such commitments are certainly the first step to establish solid and long term collaborations between the future partners of the Tropical Atlantic Monitoring/Observing System.

Also, a fundamental requirement for the success of PIRATA is the "human power" needed to ensure, in each partner's teams and laboratories, work at sea along with the sensor preparation, calibration and data treatment. This relies upon national/international contributions and funding efforts that depend on political decisions, which are tied to the importance decision-makers will give to climate change monitoring and related issues. This underscores the continued need to communicate effectively the importance of PIRATA and the Tropical Atlantic Observing System to the public and funding agencies.

8 Conclusion

Since 1997, PIRATA partners have established and efficiently sustained a moored buoy network in the tropical Atlantic to support research, operational analyses and forecasting, and climate assessments. PIRATA has vastly increased the amount of data

available from the tropical Atlantic, not only from the moorings themselves, but also from the cruises that allow for the collection of specialized shipboard data and for the deployment of Argo floats, Global Drifter Program drifters, and XBTs that help build other components of the ocean observing system. PIRATA data have proven to be valuable for constraining oceanic and atmospheric reanalysis products, for satellite validation, and for the development of new *in situ* and/or satellite/*in situ* data products. PIRATA data and data products are readily available through the Global Data Centers (Coriolis/IFREMER in France and NDBC/NOAA in the USA) and from other dedicated web databases (PIRATA, TACE, PREFACE, and others). The mooring data are also transmitted to operational centers worldwide via the Global Telecommunications System for weather, climate, ocean forecasting, real time ocean monitoring, and operational system's routine validation and verification.

The long records now available from PIRATA moorings allow studies of decadal variability and climate change, extending beyond the original intraseasonal to interannual time scale focus of the array. The very high-frequency (minutes to hours) buoy measurements on the other hand allow for process studies of the diurnal cycle and its interactions with lower frequencies, near-inertial waves, short time scale equatorial waves propagation, instability wave dynamics, and other modes of high frequency variability. PIRATA's multi-decade, multi-variate, high temporal resolution records of oceanic and surface atmospheric variables are a unique and valuable contribution to the Global Ocean Observing System (GOOS) and the Global Climate Observing System (GCOS) in the tropical Atlantic (*e.g*. Legler et al. 2015). The moorings and ships used in the program have in addition served as valuable platforms of opportunity for other programs to study, for example, ocean mixing, ocean biogeochemistry, oxygen variability and carbon cycle processes, and marine animal behavior.

PIRATA also provides opportunities for collaborative studies involving "piggyback" operations sponsored by other groups or organizations, such as sediment trap deployments from PIRATA cruise to study downward particles fluxes or deep T/S measurements on moorings as promoted by the OceanSITES program. PIRATA has long history of working in collaboratively and welcomes further involvement of self-supported activities that are consistent with PIRATA's broad mission and technically feasible.

Studies are presently going on to determine the complementarity of data sets for reanalysis of T, S, current, and other fields. Observation System Experiments and OSSEs are being conducted, notably in the framework of the EU AtlantOS project that will provide important information on the relative merits of potential priority enhancements in PIRATA (additional ocean sensors, new parameters to measure, etc). These enhancements would require new resources from the existing partner nations supporting the array and/or involvement of additional partners and programs. A *sine qua non* for moving forward however is our assertion that the existing array of 18 well-functioning and well-supported sites be the starting point for discussion of any enhancements.

PIRATA data are supplied in real-time to customers in operational weather, climate, and ocean services. Oceanic and atmospheric measurements are essential for assessing the impacts of ocean warming, sea level rise, extreme weather events, deoxygenation, ocean acidification, marine ecosystems, living marine resources, and pollution (*e.g*. Schiller et al. 2016). The methods by which one quantitatively gauges the economic value of a particular observing system component, however, is subjective at best. End users in society typically see a product that includes many different data sets assimilated into a model analysis and

forecast system. The value of such a product depends not just on the data that goes into it, but the quality of the models and assimilation systems used. In addition, data may be used in model development independent of any specific product delivered to users. Thus, while it is important to pose the question "what is the economic value of PIRATA data", it is very difficult to come up with credible answers at this point in time given the state of the art in data assimilation, ocean-atmosphere modeling, and operational forecasting.

We can nonetheless claim that since inception, PIRATA has fundamentally advanced our understanding of large-scale ocean dynamics, ocean-atmosphere interactions, and the tropical Atlantic Ocean's role in climate. It has also supported building other components of the GOOS and GCOS like Argo and the Global Drifter Program, and it feeds data every day in real time to operational weather, climate and ocean forecasting centers around the world. Finally, it has supported ocean and coupled ocean-atmosphere model development, satellite validation, and development of a wide range of oceanic and atmospheric products that are used extensively around the world. It has achieved this success because PIRATA leadership has continuously evolved the array to keep pace with changing scientific priorities and taken advantage of new technologies as they become available; and because the program is well managed with a stable base of support in three countries. Through its present status and potential enhancements, PIRATA will continue to play a key role in the future Tropical Atlantic Observing System presently under design.

Acknowledgments:

The authors acknowledge all the key contributors to the PIRATA program from its inception, *i.e.* the institutions NOAA, IRD, Météo-France, INPE, DHN; all past members of the PIRATA Resources Board and of the PIRATA Scientific Steering Group; all engineers and technicians ensuring the yearly cruises, data acquisition, data treatment and material maintenance (of NOAA, DHN and IRD's IMAGO service unit); Research Vessel crews… All PIRATA data used in this paper are made available for free through the PIRATA main website at: https://www.pmel.noaa.gov/gtmba/pmel-theme/atlantic-ocean-pirata and related linked websites. We are indebted to H. Pillar for the analysis and the figure related to near inertial waves. Part of the work was funded by the EU FP7/2007-2013 under grant agreement no. 603521, PREFACE and by the EU Horizon 2020 under grant agreement no. 2014-633211, AtlantOS. This is NOAA's Pacific Marine Environmental Laboratory (PMEL) contribution no. 4793. Some of the authors were supported by NOAA's Ocean Observing and Monitoring Division (FundRef# 100007298) and the Atlantic Oceanographic and Meteorological Laboratory (AOML). We sincerely thank Semyon Grodsky for his valuable comments and suggestions on an earlier version of this manuscript.

References:

Ascani, F., E. Firing, J. P. McCreary, P. Brandt, & R. J. Greatbatch (2015). The deep equatorial ocean circulation in wind-forced numerical solutions. *J. Phys. Oceanogr.*, *45*, 1709-1734, doi:10.1175/JPO-D-14-0171.1.

Athie, G., & F. Marin (2008). Cross-equatorial structure and temporal modulation of Intra-seasonal variability at the surface of the Tropical Atlantic Ocean. *J. Geophys. Res.*, *113*, C8, doi:10.1029/2007JC004332.

Athie, G., F. Marin, A.-M. Treguier, B. Bourlès, & C. Guiavarc'h (2009). Sensitivity of near surface Tropical Instability Waves to sub-monthly wind forcing in the tropical Atlantic. *Ocean Modell.*, *30*, 241-255.

Awo, F. M., G. Alory, C.Y. Da-Allada, T. Delcroix, J. Jouanno, E. Kestenare, & E. Baloïtcha (2018). Sea surface salinity signature of the tropical Atlantic interannual climatic modes. *J. Geophys. Res. Oceans*, *123*, 7420–7437, doi:10.1029/2018JC013837.

Bachèlery, M.-L., S. Illig, & I. Dadou (2016), Interannual variability in the South-East Atlantic Ocean, focusing on the Benguela Upwelling System: Remote versus local forcing, *J. Geophys. Res. Oceans*, *121*, 284–310, doi:10.1002/2015JC011168.

Balmaseda, M.A., F. Hernandez, A. Storto, M.D. Palmer, O. Alves, L. Shi, et al. (2015). The Ocean Reanalyses Intercomparison Project (ORA-IP), *Journal of Operational Oceanography*, 8:sup1, s80-s97, doi:10.1080/1755876X.2015.1022329.

Benetti, M., H. C. Steen-Larsen, G. Reverdin, Á. E. Sveinbjörnsdóttir, G. Aloisi, M. B. Berkelhammer, & al. (2017a). Stable isotopes in the atmospheric marine boundary layer water vapour over the Atlantic Ocean, 2012-2015, *Nature Sci. Data*, *4*, article 160128, doi:10.1038/sdata.2016.128.

Benetti, M., G. Reverdin, G. Aloisi, & Á. Sveinbjörnsdóttir (2017b). Stable isotopes in surface waters of the Atlantic Ocean: Indicators of ocean-atmosphere water fluxes and oceanic mixing processes. *J. Geophys. Res. Oceans*, *122*, 4723–4742, doi:10.1002/2017JC012712.

Berger, H., A. M. Treguier, N. Perenne, & C. Talandier (2014). Dynamical contribution to sea surface salinity variations in the eastern Gulf of Guinea based on numerical modelling. *Clim. Dyn.*, *43*, 3105-3122, doi:10.1007/s00382-014-2195-4.

Blockley, E.W., M.J. Martin, A.J. McLaren, A.G. Ryan, J. Waters, et al. (2014). Recent development of the Met Office operational ocean forecasting system: an overview and assessment of the new Global FOAM forecasts, *Geosci. Model. Dev.*, *7 (6)*, 2613-2638, doi:10.5194/gmd-7-2613-2014.

Boilley, A., and L. Wald (2015). Comparison between meteorological re-analyses from ERA-Interim and MERRA and measurements of daily solar irradiation at surface, *Renewable Energy, Elsevier*, *75*, 135-143, doi: 10.1016/j.renene.2014.09.042.

Bonou, F. K., C. Noriega, N. Lefèvre, & M. Araujo (2016). Distribution of CO_2 parameters in the Western Tropical Atlantic Ocean. *Dynamics of Atmospheres and Oceans*, *73*, 47-60, doi:10.1016/j.dynatmoce.2015.12.001.

Bourlès, B., P. Brandt, G. Caniaux, M. Dengler, Y. Gouriou, E. Key, et al. (2007). African Monsoon Multidisciplinary Analysis (AMMA): Special measurements in the Tropical Atlantic, *CLIVAR Exchanges Letters, 41 (Vol. 12, n°2), 7-9*.

Bourlès, B., R. Lumpkin, M. J. McPhaden, F. Hernandez, P. Nobre, E. Campos, et al. (2008). The PIRATA Program: History, Accomplishments, and Future Directions. *Bull. Am. Meteorol. Soc.*, *89* (8), doi:10.1175/2008BAMS2462.1.

Bourlès, B. (2016). *PREFACE EU FP7 603521 Deliverable 3.2* "Enhancing prediction of tropical Atlantic climate and its impacts: Report air-sea interactions" (https://preface.w.uib.no/output/d-and-ms/#del).

Bourlès, B., P. Brandt, & N. Lefèvre (2017). *AtlantOS EU H2020 633211 Deliverable 3.3* "Enhancement of autonomous observing networks: PIRATA network improvement report" (https://www.atlantos-h2020.eu/project-information/work-packages/deliverables/).

Bourras, D., A. Weill, G. Caniaux, L. Eymard, B. Bourlès, S. Letourneur, et al. (2009). Turbulent air-sea fluxes in the Gulf of Guinea during the EGEE-AMMA experiment. *J. Geophys. Res.*, *114*, C04014, doi:10.1029/2008JC004951.

Boutin, J., Y. Chao, W. Asher, T. Delcroix, R. Drucker, K. Drushka, & al. (2016). Satellite and In Situ Salinity: Understanding Near-Surface Stratification and Sub-footprint Variability. *Bull. Amer. Meteor. Soc.*, doi:10.1175/BAMS-D-15-00032.1.

Bowman, K. P., C. R. Homeyer, & D. G. Stone (2009). A Comparison of Oceanic Precipitation Estimates in the Tropics and Subtropics. *J. Appl. Meteor. Climatol.*, *48*, 1335–1344, doi:10.1175/2009JAMC2149.1.

Brandt, P., F. A. Schott, C. Provost, A. Kartavtseff, V. Hormann, B. Bourlès, & J. Fischer (2006). Circulation in the central equatorial Atlantic: Mean and intraseasonal to seasonal variability. *Geophys. Res. Lett., 33*(7), doi:10.1029/2005GL025498.

Brandt, P., V. Hormann , B. Bourlès, J. Fischer, F. Schott , L. Stramma, & M. Dengler (2008). Oxygen tongues and zonal currents in the equatorial Atlantic, *J. Geophys. Res., 113*, C04012, doi:10.1029/2007JC004435.

Brandt, P., G. Caniaux, B. Bourlès, A. Lazar, M. Dengler, A. Funk, et al. (2011a). Equatorial upper-ocean dynamics and their interaction with the West African Monsoon. *Atmosph. Sci. Letters*, *12*, 24-30, doi:10.1002/asl.287.

Brandt, P., A. Funk, V. Hormann, M. Dengler, R. J. Greatbatch, & J. M. Toole (2011b). Interannual atmospheric variability forced by the deep equatorial Atlantic Ocean, *Nature*, 473, 497-500, doi: 10.1038/nature10013.

Brandt, P., R. J. Greatbatch, M. Claus, S.-H. Didwischus, V. Hormann, A. Funk, et al. (2012). Ventilation of the equatorial Atlantic by the equatorial deep jets, *J. Geophys. Res., 117*, C12015, doi:10.1029/2012JC008118.

Brandt, P., A. Funk, A. Tantet, W. E. Johns & J. Fischer (2014). The Equatorial Undercurrent in the central Atlantic and its relation to tropical Atlantic variability. *Clim. Dyn., 43*(11), 2985-2997, doi:10.1007/s00382-014-2061-4.

Brandt, P., H. W. Bange, D. Banyte, M. Dengler, S. H. Didwischus, T. Fischer, et al. (2015). On the role of circulation and mixing in the ventilation of oxygen minimum zones with a focus on the eastern tropical North Atlantic, *Biogeosciences*, *12*, 489–512, doi:10.5194/bg-12-489-2015.

Brandt, P., M. Claus, R. J. Greatbatch, R. Kopte, J. M. Toole, W. E. Johns, & C. W. Böning (2016). Annual and semi-annual cycle of equatorial Atlantic circulation associated with basin mode resonance. *J. Phys. Oceanogr., 46*, 3011–3029, doi:10.1175/JPO-D-15-0248.1.

Brassington, G.B., M.J. Martin, H.L. Tolman, S. Akella, M.A. Balmaseda, C.R.S. Chambers, et al. (2015). Progress and challenges in short- to medium-range coupled prediction, *Journal of Operational Oceanography, 8 (sup2)*, s239-s258, 10.1080/1755876X.2015.1049875.

Bruto, L., M. Araujo, C. Noriega, D. Veleda, & N. Lefèvre (2017). Variability of CO2 fugacity at the western edge of the tropical Atlantic Ocean from the 8°N to 38°W PIRATA buoy. *Dyn. Atmos. Oceans, 78*, 12017, doi:10.1016/j.dynatmoce.2017.01.003.

Bunge, L., C. Provost, B. L. Hua, & A. Kartavtseff (2008). Variability at intermediate depths at the equator in the Atlantic Ocean in 2000–06: annual cycle, equatorial deep jets, and intraseasonal meridional velocity fluctuations. *J. Phys. Oceanogr., 38*, 1794–1806. doi:10.1175/2008JPO3781.1.

Burmeister, K., P. Brandt, & J. F. Lübbecke (2016). Revisiting the cause of the eastern equatorial Atlantic cold event in 2009. *J. Geophys. Res. Oceans, 121*, 4777–4789, doi:10.1002/2016JC011719.

Cabanes, C., A. Grouazel, K. von Schuckmann, M. Hamon, V. Turpin, C. Coatanoan, et al. (2013). The CORA dataset: validation and diagnostics of in-situ ocean temperature and salinity measurements, *Ocean Sci., 9* (1), 1-18, 10.5194/os-9-1-2013.

Camara, I., N. Kolodziejczyk, J. Mignot, A. Lazar, & A. T. Gaye (2015). On the seasonal variations of salinity of the tropical Atlantic mixed layer. *J. Geophys. Res., 120*, 4441-4462, doi:10.1002/2015JC010865.

Campos, E., C. A. S. França, N. Vicentini, L. Francisco, L. V. Nonnato, A. R. Piola, et al. (2014). Atlas-B: Development and Testing of a Brazilian Deep-Ocean Moored Buoy for Climate Research. *J. Shipping and Ocean Engineering, 2*, 11-20.

Caniaux, G., H. Giordani, J. L. Redelsperger, F. Guichard, E. Key, & M. Wade (2011). Coupling between the Atlantic Cold Tongue and the West African Monsoon in boreal Spring and Summer. *J. Geophy. Res., 116*, C04003, doi:10.1029/2010JC006570.

Carton, J. A., & Z. X. Zhou (1997). Annual cycle of sea surface temperature in the tropical Atlantic Ocean. *J. Geophys. Res., 102*, 27,813-27,824.

Castellanos, P., E. Campos, I. Giddy, & W. Santis (2016). Inter-comparison studies between high-resolution HYCOM simulation and observational data: the South Atlantic and the Agulhas Leakage system. *J. Mar. Sys.*, *159*, 76-88, doi: 10.1016/j.jmarsys.2016.02.010.

Castellanos, P., E. J. D. Campos, J. Piera, O. T. Sato, & M. A. F. Silva Dias (2017). Impacts of the Agulhas Leakage on the Tropical Atlantic Western Boundary Systems. *J. Clim., 30*, 6645-6659, doi:10.1175/JCLI-D-15-087.s1.

Chang, P., T. Yamagata, P. Schopf, S.K. Behera, J. Carton, W. E. Kessler, et al. (2006). Climate fluctuations of Tropical Coupled Systems – The Role of Ocean Dynamics. *J. Climate (Special Section), 19*, 5122-5174, doi :10.1175/JCLI3903.1.

Cintra, M., C. Lentini, J. Servain, M. Araujo, & E. Marone (2015). Physical processes that drive the seasonal evolution of the Southwestern Tropical Atlantic Warm Pool. *Dyn. Atmos. Ocean, 72*, 1-11, doi:10.1016/j.dynatmoce.2015.08.001.

Claus, M., R. J. Greatbatch, P. Brandt, & J. M. Toole (2016). Forcing of the Atlantic equatorial deep jets derived from observations, *J. Phys. Oceanogr*., *46*, 3549-3562, doi: 10.1175/JPO-D-16-0140.1.

Clayson, C. A., & D. Weitlich (2007). Variability of tropical diurnal sea surface temperature. *J. Climate*, *20*, 334-352, doi :10.1175/JCLI3999.1.

Cole, R., L. Barreira, & E. Campos (2013). Development and Deployment of Brazil's First Buoy System. *Marine Technology Reporter*, 46-51.

Coles, V. J., M. T. Brooks, J. Hopkins, M. R. Stukel, P. L. Yager, & R. R. Hood (2013): The pathways and properties of the Amazon River Plume in the tropical North Atlantic Ocean. *J. Geophys. Res*., *118*, doi:10.1002/2013JC008981.

Da-Allada, C. Y., G. Alory, Y. du Penhoat, E. Kestenare, F. Durand, & N. M. Hounkonnou (2013). Seasonal mixed-layer salinity balance in the tropical Atlantic Ocean: Mean state and seasonal cycle. *J. Geophys. Res*., *118*, 332-345, doi:10.1029/2012JC008357.

Da-Allada, C. Y., Y. du Penhoat, J. Jouanno, G. Alory, & N. M. Hounkonnou (2014). Modeled mixed-layer salinity balance in the Gulf of Guinea: seasonal and interannual variability. *Ocean Dyn*., *64*, 1783-1802, doi:10.1007/s10236-014-0775-9.

Da-Allada, C. Y., J. Jouanno, F. Gaillard, N. Kolodziejczyk, C. Maes, N. Reul, & B. Bourlès (2017). Importance of the Equatorial Undercurrent on the sea surface salinity in the eastern equatorial Atlantic in boreal spring. *J. Geophys. Res. Oceans*, *122*, 521–538, doi :10.1002/2016JC012342.

Danuor, S., A. Gaye, H. Yakouba, A. Mariko, M. I. Bouzou, M. Maiga, et al. (2011). Education in meteorology and climate sciences in West Africa, *Atmos. Sci. Let., 12(1)*, 155-159, doi:10.1002/asl.326.

De Coëtlogon, G., S. Janicot, & A. Lazar (2010). Intraseasonal variability of the ocean – atmosphere coupling in the Gulf of Guinea during boreal spring and summer. *Q. J. R. Meteorol. Soc., 136*, 426–441, doi:10.1002/qj.554.

Dohan, K., & R. E. Davis (2011). Mixing in the Transition Layer during Two Storm Events. *J. Phys. Oceanogr*., *41*, 42-66.

Doi, T., T. Tozuka, & T. Yamagata (2010). The Atlantic Meridional Mode and Its Coupled Variability with the Guinea Dome. *J. Climate, 23*, 455–475, doi:10.1175/2009JCLI3198.1.

Fischer, T., D. Banyte, P. Brandt, M. Dengler, G. Krahmann, T. Tanhua, & M. Visbeck (2013). Diapycnal oxygen supply to the tropical North Atlantic oxygen minimum zone, *Biogeosciences*, *10*, 5079–5093, doi:10.5194/bg-10-5079-2013.

Florenchie, P., J. R. E. Lutjeharms, C. J. C. Reason, S. Masson, & M. Rouault (2003). The source of Benguela Niños in the South Atlantic Ocean. *Geophys. Res. Lett., 30*, 10–13, doi:10.1029/2003GL017172.

Foltz, G. R., S. A. Grodsky, J. A. Carton, & M. J. McPhaden (2003). Seasonal mixed layer heat budget of the tropical Atlantic Ocean. *J. Geophys. Res., 108*, 3146, doi:10.1029/2002JC001584.

Foltz, G.R. & M. J. McPhaden (2006a). The role of oceanic heat advection in the evolution of tropical North and South Atlantic SST anomalies. *J. Climate, 19*, 6122-6138.

Foltz, G.R. & M. J. McPhaden (2006b). Unusually warm sea surface temperatures in the tropical North Atlantic during 2005. *Geophys. Res. Lett., 33*, L19703, doi:10.1029/2006GL027394.

Foltz, G. R., & M. J. McPhaden (2008). Seasonal mixed layer salinity balance of the tropical North Atlantic Ocean. *J. Geophys. Res. Oceans*, 113, C02013, doi:10.1029/2007JC004178.

Foltz, G. R., & M. J. McPhaden (2009). Impact of barrier layer thickness on SST in the central tropical North Atlantic. *J. Climate*, *22*, 285-299, doi:10.1175/2008JCLI2308.1.

Foltz, G., & M. J. McPhaden (2010a). Abrupt equatorial wave-induced cooling of the Atlantic cold tongue in 2009. *Geophys. Res. Lett.*, *37 (24*), doi:10.1029/2010gl045522.

Foltz, G. R., & M. J. McPhaden (2010b). Interaction between the Atlantic meridional and Nino modes. *Geophys. Res. Lett*., L18604, doi:10.1029/2010GL044001.

Foltz, G. R., M. J. McPhaden, & R. Lumpkin (2012). A strong Atlantic Meridional Mode event in 2009: The role of mixed layer dynamics. *J. Climate*, *25*, 363-380, doi: 10.1175/JCLI-D-11-00150.1.

Foltz, G. R., C. Schmid, & R. Lumpkin (2013). Seasonal cycle of the mixed layer heat budget in the northeastern tropical Atlantic Ocean. *J. Climate*, *26*, 8169-8188, doi:10.1175/JCLI-D-13-00037.1.

Foltz, G. R., C. Schmid, & R. Lumpkin (2015). Transport of surface freshwater from the equatorial to the subtropical North Atlantic Ocean. *J. Phys. Oceanogr*., *45*, 1086-1102, doi:10.1175/JPO-D-14-0189.1.

Foltz, G. R., C. Schmid, & R. Lumpkin (2018). An enhanced PIRATA data set for tropical Atlantic ocean-atmosphere research. *J. Climate*, *31(4)*, 1499-1524, doi:10.1175/JCLI-D-16-0816.1.

Fournier, S., D. Vandemark, L. Gaultier, T. Lee, B. Jonsson, & M. M. Gierach (2017). Interannual variation in offshore advection of Amazon-Orinoco plume waters: Observations, forcing mechanisms, and impacts. *J. Geophys. Res*., *122*, 8966-8982. doi:10.1002/2017JC013103.

Freeman, E., S. D. Woodruff, S. J. Worley, S. J. Lubker, E. C. Kent, W. E. Angel, et al. (2017). ICOADS Release 3.0: a major update to the historical marine climate record. *Int. J. Climatol*., doi:10.1002/joc.4775.

Frölicher, T. L., F. Joos, G. K. Plattner, M. Steinacher, & S. C. Doney (2009). Natural variability and anthropogenic trends in oceanic oxygen in a coupled carbon cycle-climate model ensemble, *Global Biogeochem. Cy*., *23*, 15, GB1003, doi:10.1029/2008gb003316.

Gaillard, F., D. Diverres, S. Jacquin, Y. Gouriou, J. Grelet, M. Le Menn, et al. (2015). Sea surface temperature and salinity from French research vessels, 2001–2013. *Sci. Data*, 2:150054, doi: 10.1038/sdata.2015.54.

Gehlen, M., N. Gruber, R. Gangstø, L. Bopp, & A. Oschlies (2011). Biogeochemical consequences of ocean acidification and feedbacks to the earth system, in *Ocean Acidification, edited by J.-P. Gattuso, and L. Hansson, Oxford University Press*, Oxford, UK, 230-248.

Gehlen, M., R. Barciela, L. Bertino, P. Brasseur, M. Butenschön, F. Chai, et al. (2015). Building the capacity for forecasting marine biogeochemistry and ecosystems: recent advances and future developments, *J. Operation. Oceanogr.*, *8 (sup1*), s168-s187, 10.1080/1755876X.2015.1022350.

Giarolla, E., P. Nobre, M. Malagutti, & P. Pezzi (2005). The Atlantic Equatorial Undercurrent: PIRATA observations and simulations with GFDL Modular Ocean Model at CPTEC, *Geophys. Res. Lett., 32*, L10617, doi :10.1029/2004GL022206.

Giarolla, E., L. S. P. Siqueira, M. J. Bottino, M. Malagutti, V. B. Capistrano, & P. Nobre (2015). Equatorial Atlantic Ocean dynamics in a coupled ocean–atmosphere model simulation. *Ocean Dynamics*, *65* (6), 831-843.

Giordani, H., & G. Caniaux (2011). Diagnosing Vertical Motion in the Equatorial Atlantic. *Ocean Dynamics*, *61*, 1996-2018, doi:10.1007/s10236-011-0467-7.

Giordani, H., G. Caniaux, & A. Voldoire (2013). Intraseasonal mixed-layer heat budget in the equatorial Atlantic during the cold tongue development in 2006. *J. Geophys. Res., 118*, 650-671, doi:10.1029/2012JC008280.

Good, S. A., M. J. Martin, & N. A. Rayner (2013). EN4: Quality controlled ocean temperature and salinity profiles and monthly objective analyses with uncertainty estimates, *J. Geophys. Res. Oceans*, *118*, 6704–6716, doi:10.1002/2013JC009067.

Gouriou, Y., C. Andrié, B. Bourlès, S. Freudenthal, S. Arnault, A. Aman, et al. (2001). Deep circulation in the equatorial Atlantic Ocean. *Geophys. Res. Lett*., *28*, 819–822, doi:10.1029/2000GL012326.

Greatbatch, R. J., M. Claus, P. Brandt, J.-D. Matthießen, F. P. Tuchen, F. Ascani, et al. (2018). Evidence for the maintenance of slowly varying equatorial currents by intraseasonal variability, *Geophys. Res. Lett., 45*, 1923–1929, doi: 10.1002/2017GL076662.

Gregg, M. C., H. Peters, J. C. Wesson, N. S. Oakey, & T. J. Shay (1985). Intensive measurements of turbulence and shear in the equatorial undercurrent. *Nature*, *318*, 140–144.

Grodsky, S. A., J. A. Carton, C. Provost, J. Servain, J. A. Lorenzzetti, & M. J. McPhaden (2005). Tropical instability waves at 0°N, 23°W in the Atlantic: A case study using Pilot Research Moored Array in the Tropical Atlantic (PIRATA) mooring data, *J. Geophys. Res*., *110*, C08010, doi:10.1029/2005JC002941.

Grodsky, S. A., and J. A. Carton (2006), Influence of the tropics on the climate of the South Atlantic, *Geophys. Res. Lett.*, *33*, L06719, doi:10.1029/2005GL025153.

Grodsky, S. A., J. A. Carton, and C. R. McClain (2008), Variability of upwelling and chlorophyll in the equatorial Atlantic, *Geophys. Res. Lett.*, *35*, L03610, doi:10.1029/2007GL032466.

Grodsky, S. A., J. A. Carton, & F. O. Bryan (2014). A curious local surface salinity maximum in the northwestern tropical Atlantic. *J. Geophys. Res*., 484-495, doi:10.1002/2013JC009450.

Hahn, J., P. Brandt, R. J. Greatbatch, G. Krahmann & A. Körtzinger (2014). Oxygen variance and meridional oxygen supply in the Tropical North East Atlantic oxygen minimum zone. *Clim. Dyn*., *43(11)*, 2999-3024, doi:10.1007/s00382-014-2065-0.

Hahn, J., P. Brandt, S. Schmidtko, & G. Krahmann (2017). Decadal oxygen change in the eastern tropical North Atlantic. *Ocean Sci.*, *13*, 551-576, doi:10.5194/os-13-551-2017.

Hastenrath, S. (1977). Hemispheric asymmetry of oceanic heat budget in the equatorial Atlantic and eastern Pacific. *Tellus*, *29*, 523-529.

Helm, K. P., N. L. Bindoff, & J. A. Church (2011). Observed decreases in oxygen content of the global ocean, *Geophys. Res. Lett*., *38*, L23602, doi:10.1029/2011gl049513.

Henocq, C., J. Boutin, G. Reverdin, F. Petitcolin, S. Arnault, & P. Lattes (2010). Vertical Variability of Near-Surface Salinity in the Tropics: Consequences for L-Band Radiometer Calibration and Validation. *J. Atmos. Oceanic Technol*., *27*, 192–209, doi:10.1175/2009JTECHO670.1.

Herbert, G., B. Bourlès, P. Penven, & J. Grelet (2016). New insights on the upper layer circulation north of the Gulf of Guinea. *J. Geophys. Res. Oceans*, *121*, 6793–6815, doi:10.1002/2016JC01195.

Herbert G., & B. Bourlès (2018). Impact of intraseasonal wind bursts on sea surface temperature variability in the far Eastern tropical Atlantic Ocean during boreal spring 2005 and 2006: focus on the mid-May 2005 event, *Ocean Sciences*, 14, 849–869, doi:10.5194/os-14-849-2018.

Hernandez, F., E. Blockley, G. B. Brassington, F. Davidson, P. Divakaran, M. Drévillon, et al. (2015). Recent progress in performance evaluations and near real-time assessment of operational ocean products, *Journal of Operational Oceanography*, *8 (sup2)*, s221-s238, doi:10.1080/1755876X.2015.1050282.

Hernandez, O., J. Jouanno, V. Echevin, & O. Aumont (2017). Modification of sea surface temperature by chlorophyll concentration in the Atlantic upwelling systems, *J. Geophys. Res. Oceans*, *122*, 5367–5389, doi:10.1002/2016JC012330.

Hormann, V., & P. Brandt (2007). Atlantic Equatorial Undercurrent and associated cold tongue variability, *J. Geophys. Res*., *112*, C06017, doi:10.1029/2006JC003931.

Hormann, V., & P. Brandt (2009). Upper equatorial Atlantic variability during 2002 and 2005 associated with equatorial Kelvin waves. *J. Geophys. Res.*, *114*, C03007, doi:10.1029/2008JC005101.

Hounsou-Gbo, G. A., M. Araujo, B. Bourlès, D. Veleda, & J. Servain (2015). Tropical Atlantic contributions to strong rainfall variability along the Northeast Brazilian coast. *Advances in Meteorology*, *vol. 2015*, Article ID 902084, doi:10.1155/2015/902084.

Hu, Z.-Z., A. Kumar, B. Huang, & J. Zhu (2013). Leading Modes of the Upper-Ocean Temperature Interannual Variability along the Equatorial Atlantic Ocean in NCEP GODAS. *J. Climate*, *26*, 4649–4663, http://dx.doi.org/10.1175/JCLI-D-12-00629.1.

Hummels, R., M. Dengler, & B. Bourlès (2013). Seasonal and regional variability of upper ocean diapycnal heat flux in the Atlantic cold tongue, *Prog. Oceanogr*., *111*, 52-74, doi:10.1016/j.pocean.2012.11.001.

Hummels, R., M. Dengler, P. Brandt, & M. Schlundt (2014). Diapycnal heat flux and mixed layer heat budget within the Atlantic cold tongue. *Clim. Dyn*., *43*, 3179-3199, doi:10.1007/s00382-014-2339-6.

Imbol Koungue, R. A., S. Illig, & M. Rouault (2017). Role of interannual Kelvin wave propagations in the equatorial Atlantic on the Angola Benguela Current system. *J. Geophys. Res. Oceans*, *122*, 4685–4703, doi:10.1002/2016JC012463.

Jochum, M. P. Malanotte-Rizzoli, & A. Busalacchi (2004). Tropical Instability Waves in the Atlantic Ocean., *Ocean Modell., 7*, 145-163

Jochum, M., B. Briegleb, G. Danabasoglu, W. Large, N. Norton, S. Jayne, et al. (2013). The impact of oceanic near-inertial waves on climate. *J. Clim., 26*, 2833–2844.

Jochum, M. (2017). *PREFACE EU FP7 603521 Deliverable 3.3* "Enhancing prediction of tropical Atlantic climate and its impacts : Report on Near Inertial Waves" (https://preface.w.uib.no/output/d-and-ms/#del).

Johns, W. E., P. Brandt, & P. Chang (2014a). Tropical Atlantic variability and coupled model climate biases: results from the Tropical Atlantic Climate Experiment (TACE). *Clim. Dyn., 43*(11*)*, 2887, doi:10.1007/s00382-014-2392-1.

Johns, W. E., P. Brandt, B. Bourlès, A. Tantet, A. Papapostolou & A. Houk (2014b). Zonal Structure and Seasonal Variability of the Atlantic Equatorial Undercurrent. *Clim. Dyn., 43*(11), 3047-3069, doi:10.1007/s00382-014-2136-2.

Jouanno, J., F. Marin, Y. duPenhoat, J. Sheinbaum, & J. Molines (2011). Seasonal heat balance in the upper 100 m of the Equatorial Atlantic Ocean. *J. Geophys. Res., 116*, C09003, doi:10.1029/2010JC006912.

Jouanno, J., F. Marin, Y. Du Penhoat, & J.M. Molines (2013). Intraseasonal modulation of the surface cooling in the Gulf of Guinea. *J. Phys. Oceanogr., 43* (2), doi:10.1175/JPO-D-12-053.1.

Jouanno, J., O. Hernandez, E. Sanchez-Gomez, & B. Deremble (2017). Equatorial Atlantic interannual variability and its relation to dynamic and thermodynamic processes, *Earth Syst. Dyn., 8*, 1061–1069, doi:10.5194/esd-8-1061-2017.

Kara, A. B., & C. N. Barron (2007). Fine-resolution satellite-based daily sea surface temperatures over the global ocean. *J. Geophys. Res., 112*, C05041, doi:10.1029/2006JC004021.

Karstensen, J., L. Stramma, & M. Visbeck (2008). Oxygen minimum zones in the eastern tropical Atlantic and Pacific oceans. *Progr. Oceanogr., 77*, 331-350, doi:10.1016/j.pocean.2007.05.009 .

Karstensen, J., B. Fiedler, F. Schütte, P. Brandt, A. Körtzinger, G. Fischer, et al. (2015). Open ocean dead zones in the tropical North Atlantic Ocean, *Biogeosciences, 12*, 2597–2605, doi:10.5194/bg-12-2597-2015 .

Keeling, R. F., A. Körtzinger, & N. Gruber (2010). Ocean deoxygenation in a warming world, *Annu. Rev. Mar. Sci., 2*, 199–229, doi:10.1146/annurev.marine.010908.163855.

Koffi, U., N. Lefèvre, G. Kouadio, & J. Boutin (2010). Surface CO_2 parameters and air-sea CO_2 flux distribution in the eastern equatorial Atlantic Ocean. *J. Mar. Syst., 82*, 135-144.

Kolodziejczyk, N., B. Bourlès, F. Marin, J. Grelet & R. Chuchla (2009). The seasonal variability of the Equatorial Undercurrent and the South Equatorial Undercurrent at 10°W as inferred from recent in situ observations, *J. Geophys. Res., 114*, C06014, doi :10.1029/2008JC004976.

Kolodziejczyk, N., F. Marin, B. Bourlès, Y. Gouriou, & H. Berger (2014). Seasonal variability of the Equatorial Undercurrent termination and associated salinity maximum in the Gulf of Guinea. *Clim. Dyn., 43 (11)*, 3025-2046, doi:10.1007/s00382-014-2107-7.

Kolodziejczyk, N., O. Hernandez, J. Boutin & G. Reverdin (2015). SMOS salinity in the subtropical North Atlantic salinity maximum: 2. Two-dimensional horizontal thermohaline variability. *J. Geophys. Res., 120*,972-987, doi :10.1002/2014JC010103.

Kolodziejczyk, N., A. Prigent-Mazella, & F. Gaillard (2017). ISAS-15 temperature and salinity gridded fields. SEANOE, doi:10.17882/52367.

Large, W. G., & S.G. Yeager (2009). Global climatology of an interannually varying air–sea flux data set. *Clim. Dyn., 33 (2-3)*, 341-364, doi:10.1007/s00382-008-0441-3.

Lea, D. J., M. J. Martin, & P. R. Oke (2014). Demonstrating the complementarity of observations in an operational ocean forecasting system, *Q. J. R. Meteorol. Soc., 140 (683)*, 2037-2049, doi :10.1002/qj.2281.

Leduc-Leballeur, M., L. Eymard, & G. de Coëtlogon (2011). Observation of the marine atmospheric boundary layer in the Gulf of Guinea during the 2006 boreal spring. *Q. J. R. Meteorol. Soc., 137*, 992–1003, doi:10.1002/qj.808.

Lee, T., G. Lagerloef, H.-Y. Kao, M. J. McPhaden, J. Willis, & M. M. Gierach (2014). The influence of salinity on tropical Atlantic instability waves. *J. Geophys. Res. Oceans, 119*, 8375–8394, doi :10.1002/2014JC010100.

Lefèvre, N., A. Guillot, L. Beaumont, & T. Danguy (2008). Variability of fCO2 in the Eastern

Tropical Atlantic from a moored buoy. *J. Geophys. Res.*, *113*, C01015, doi:10.1029/2007JC004146.
Lefèvre, N. (2009). Low CO_2 concentrations in the Gulf of Guinea during the upwelling season in 2006. *Marine Chemistry, 113*, 93-101.
Lefèvre, N., & L. Merlivat (2012). Carbon and oxygen net community production in the eastern tropical Atlantic estimated from a moored buoy. *Global Biogeochem. Cycles, 26*, GB1009, doi:10.1029/2010GB004018.
Lefèvre, N., D. F. Urbano, F. Gallois & D. Diverrès (2014). Impact of physical processes on the seasonal distribution of CO_2 in the western tropical Atlantic. *J. Geophys. Res. 119*, doi: 10.1002/2013JC009248.
Lefèvre N., D. Veleda, M. Araujo, & G. Caniaux (2016). Variability and trends of carbon parameters at a time-series in the Eastern Tropical Atlantic. *Tellus B, 68*, doi:10.3402/tellusb.v68.30305.
Legler, D., H. J. Freeland, R. Lumpkin, G. Ball, M. J. McPhaden, S. North, et al. (2015). The current status of the real-time in situ global ocean observing system for operational oceanography. *J. Operational Oceanography, 8 (S2)*, 189-200, doi:10.1080/1755876X.2015.1049883.
Lehodey, P., A. Conchon, I. Senina, R. Domokos, B. Calmettes, J. Jouanno, et al. (2015). Optimization of a micronekton model with acoustic data. – *ICES J. Mar. Sci.*, *72(5*), 1399-1412.
Lellouche, J.-M., O. Le Galloudec, M. Drévillon, C. Régnier, E. Greiner, G. Garric, et al. (2013). Evaluation of global monitoring and forecasting systems at Mercator Océan, *Ocean Sci*., *9 (1)*, 57-81, 10.5194/os-9-57-2013.
Le Quéré, C., R. M. Andrew, P. Friedlingstein, S. Sitch, J. Pongratz, A. C. Manning, et al. (2018). Global Carbon Budget 2017, *Earth Syst. Sci. Data, 10(1)*, 405–448, doi:10.5194/essd-10-405-2018.
Lien, R.-C., D. R. Caldwell, M. C. Gregg, & J. N. Moum (1995). Turbulence variability in the central Pacific at the beginning of the 1991–93 El Niño. *J. Geophys. Res. 100*, 6881–6898.
Liu, C., R. P. Allan, M. Mayer, P. Hyder, N. G. Loeb, C. D. Roberts, et al. (2017). Evaluation of satellite and reanalysis-based global net surface energy flux and uncertainty estimates. *J. Geophys. Res. Atmos*., *122*, 6250–6272, doi:10.1002/2017JD026616.
Lübbecke, J. F., C. W. Böning, N. S. Keenlyside, & S. P. Xie (2010). On the connection between Benguela and equatorial Atlantic Niños and the role of the South Atlantic Anticyclone. *J. Geophys. Res. Ocean.*, *115*, 1–16, doi:10.1029/2009JC005964.
Lübbecke, J., & M. J. McPhaden (2013). A comparative stability analysis of Atlantic and Pacific Niño modes. *J. Climate, 26*, 5965-5980, doi:10.1175/JCLI-D-12-00758.1.
Lutz, K., J. Jacobeit, & J. Rathmann (2015). Atlantic warm and cold water events and impact on African west coast precipitation. *Int. J. Clim.*, *35*(1), 128-141.
Luyten, J. R., J. Pedlosky, & H. Stommel (1983). The Ventilated Thermocline, *J. Phys. Oceanogr.*, *13*, *292–309*, doi:10.1175/1520-0485(1983)013<0292:tvt>2.0.co;2.
Marin, F., G. Caniaux, B. Bourlès, H. Giordani, Y. Gouriou, & E. Key (2009). Why were sea surface temperatures so different in the eastern equatorial Atlantic in June 2005 and 2006? *J. Phys. Oceanogr*., *39*, 1416-1431, doi:10.1175/2008JPO4030.1.
Marullo, S., R. Santoleri, V. Banzon, R. H. Evans, & M. Guarracino (2010). A diurnal-cycle resolving sea surface temperature product for the tropical Atlantic. *J. Geophys. Res*., *115*, C05011, doi:10.1029/2009JC005466.
Masina, S., A. Storto, N. Ferry, M. Valdivieso, K. Haines, et al. (2015). An ensemble of eddy-permitting global ocean reanalyses from the MyOcean project, *Clim. Dyn.*, 1-29, doi:10.1007/s00382-015-2728-5.
McPhaden, M. J., A. J. Busalacchi, R. Cheney, J. R. Donguy, K. S. Gage, D. Halpern, et al. (1998). The Tropical Ocean-Global Atmosphere (TOGA) observing system: A decade of progress. *J. Geophys. Res., 103*, 14,169-14,240.
Merle, J. (1980). Seasonal heat budget in the equatorial Atlantic Ocean. *J. Phys. Oceanogr*., *10*, 464-469.
Meynadier, R., G. de Coëtlogon, S. Bastin, L. Eymard & S. Janicot (2015). Sensitivity testing of WRF parameterizations on air–sea interaction and its impact on water cycle in the Gulf of Guinea, *Q. J. R. Meteorol. Soc. 141*, 1804–1820, doi:10.1002/qj.2483.
Meynadier R., G. de Coëtlogon, S. Bastin, L. Eymard & S. Janicot (2016). Seasonal influence of the sea surface temperature on the low atmospheric circulation and precipitation in the eastern equatorial Atlantic, *Clim. Dyn*., *47*, 1127–1142, doi:10.1007/s00382-015-2892-7.

Molinari, R. L., J. F. Festa, & E. Marmolejo (1985). Evolution of sea surface temperature in the tropical Atlantic Ocean during FGGE, 1979, 2. Oceanographic fields and heat balance of the mixed layer. *J. Mar. Res*., *43*, 67-81.

Morris, V., P. Clemente-Colon, N. Nalli, E. Joseph, R. Armstrong, Y. Detres, et al. (2006). Measuring Trans-Atlantic Aerosol Transport from Africa. *Eos*, Dec 12, 2006, 565-566, 2006.

Moum, J. N., & D. R. Caldwell (1985). Local influences on shear flow turbulence in the equatorial ocean. *Science, 230*, 315–316.

Moum, J. N., D. R. Caldwell, & C. A. Paulson (1989). Mixing in the equatorial surface-layer and thermocline. *J. Geophys. Res. Oceans, 94*, 2005–2021

Moum, J. N., R.-C. Lien, A. Perlin, J. D. Nash, M. C. Gregg, & P. J. Wiles (2009). Sea surface cooling at the Equator by subsurface mixing in tropical instability waves. *Nature Geosci. 2*, 761–765.

Moum, J. N., A. Perlin, J. D. Nash, & M. J. McPhaden (2013). Seasonal sea surface cooling in the equatorial Pacific cold tongue controlled by ocean mixing. *Nature*, *500*, 64-67, doi:10.1038/nature12363.

Nalli, N. R., E. Joseph, V. Morris, C. Barnet, W. Wolf, D. Wolfe, et al. (2011). Multi-year observations of the tropical Atlantic atmosphere: Multidisciplinary applications of the NOAA Aerosols and Ocean Science Expeditions (AEROSE). *Bull. Amer. Meteor. Soc.*, 92, 765–789, doi :10.1175/2011BAMS2997.1.

Nobre, P., R. A. De Almeida, M. Malagutti, & E. Giarolla (2012). Coupled Ocean-Atmosphere Variations over the South Atlantic Ocean. *J. Clim., 25*, 6349-6358, doi:10.1175/JCLI-D-11-00444.1.

Nogueira Neto, A. V., H. Giordani, G. Caniaux & M. Araujo (2018). Seasonal and interannual mixed layer heat budget variability in the western tropical Atlantic from Argo floats (2007-2012), *J. Geophys. Res*., *123*, 5298-5322, doi:10.1029/2017JC013436.

Oke, P. R., G. Larnicol, E. M. Jones, V. H. Kourafalou, A. K. Sperrevik, F. Carse, et al. (2015). Assessing the impact of observations on ocean forecasts and reanalyses: Part 2, Regional applications, *J. Operat. Oceanogr*., *8 (sup1)*, s63-s79, doi:10.1080/1755876X.2015.1022080.

Okumura, Y., & S. P. Xie (2006). Some Overlooked Features of Tropical Atlantic Climate Leading to a New Niño-Like Phenomenon. *J. Climate*, *19*, 5859–5874, http://dx.doi.org/10.1175/JCLI3928.1.

Padin, X. A., M. Vázquez-Rodríguez, M. Castaño, A. Velo, F. Alonso-Pérez, J. Gago, et al. (2010). Air-Sea CO2 fluxes in the Atlantic as measured during boreal spring and autumn, *Biogeosciences, 7(5)*, 1587–1606, doi:10.5194/bg-7-1587-2010.

Parard, G., N. Lefèvre, & J. Boutin (2010). Sea water fugacity of CO_2 at the PIRATA mooring at 6ºS, 10ºW. *Tellus B, 62*, 5, 636-648.

Parard, G., J. Boutin, Y. Cuypers, P. Bouruet-Aubertot, & G. Caniaux (2014). On the physical and biogeochemical processes driving the high frequency variability of CO2 fugacity at 6°S, 10°W: Potential role of the internal waves. *J. Geophys. Res.*, *119*, 8357–8374, doi:10.1002/2014JC009965

Patricola, C.M., M. Li, Z. Xu, P. Chang, R. Saravanan, & J.-S. Hsieh (2012). An investigation of tropical Atlantic bias in a high-resolution coupled regional climate model. *Clim. Dyn.*, *39*, 2443–2463.

Peng, G., H-M Zhang, H. P. Frank, J.-R. Bidlot, M. Higaki, S. Stevens, & W. R. Hankins (2013). Evaluation of Various Surface Wind Products with OceanSITES Buoy Measurements. *Wea. Forecasting, 28*, 1281–1303, doi:10.1175/WAF-D-12-00086.1.

Perez, R. C., R. Lumpkin, W. E. Johns, G. R. Foltz, & V. Hormann (2012). Interannual variations of Atlantic tropical instability waves. *J. Geophys. Res*., *117*, C03011, doi:10.1029/2011JC007584.

Perez, R., V. Hormann, R. Lumpkin, P. Brandt, W. E. Johns, F. Hernandez, et al. (2014). Mean meridional currents in the central and eastern equatorial Atlantic. *Clim. Dyn.*, *43*(11), 2943-2962, doi :10.1007/s00382-013-1968-5.

Peter, A., M. L. Henaff, Y. du Penhoat, C. Menkes, F. Marin, J. Vialard, et al. (2006). A model study of the seasonal mixed layer heat budget in the equatorial Atlantic. *J. Geophys. Res.*, *111*, C06014.

Pham, H. T., S. Sarkar, & K. B. Winters (2013). Large-eddy simulation of deep-cycle turbulence in an equatorial undercurrent model, *J. Phys. Oceanogr*., *43*, doi:10.1175/JPO-D-13-016.1.

Pinker, R. T., H. Wang, & S. A. Grodsky (2009). How good are ocean buoy observations of radiative fluxes? *Geophys. Res. Lett*., *36*, L10811, doi :10.1029/2009GL037840.

Planton, Y., A. Voldoire, H. Giordani, & G. Caniaux (2018). Main processes of the Atlantic cold tongue interannual variability, *Clim. Dyn.*, *50*, 1495-1512, doi: 10.1007/s00382-017-3701-2.

Poli, P. (2018). Note on the impact of meteorological data from PIRATA moorings on global weather forecasts, doi:10.5281/zenodo.1164620.

Prakash, S., C. Mahesh, R. M. Gairola, & S. Pokhrel (2011). Surface Freshwater Flux Estimation Using TRMM Measurements Over the Tropical Oceans. *Atmospheric and Climate Sciences, 01:04*, 225-234, doi:10.4236/acs.2011.14025.

Prakash, S., C. Mahesh, & R. M. Gairola (2013). Comparison of TRMM Multi-satellite Precipitation Analysis (TMPA)-3B43 version 6 and 7 products with rain gauge data from ocean buoys. *Remote Sensing Lett.*, *4 (7)*, 677-685, doi:10.1080/2150704X.2013.783248.

Praveen Kumar, B., J. Vialard, M. Lengaigne, V. S. N. Murty, & M. J. McPhaden (2012). TropFlux: Air-Sea Fluxes for the Global Tropical Oceans: Description and evaluation. *Clim. Dynamics*, *38*, 1521-1543, doi:10.1007/s00382-011-1115-0.

Praveen Kumar, B., J. Vialard, M. Lengaigne, V. S. N. Murty, M. J. McPhaden, M. F. Cronin, et al. (2013). TropFlux wind stresses over the tropical oceans: evaluation and comparison with other products. *Clim. Dynamics*, *40*, 2049-2071, doi:10.1007/s00382-012-1455-4.

Reason, C. J. C., & M. Rouault (2006). Sea surface temperature variability in the tropical southeast Atlantic Ocean and West African rainfall. *Geophys. Res. Lett.*, *33*, L21705, doi:10.1029/2006GL027145.

Reverdin, G., E. Kestenare, C. Frankignoul & T. Delcroix (2007). Surface salinity in the Atlantic Ocean (30°S–50°N), *Progr. Oceanogr*., *73*, 311–340, doi:10.1016/j.pocean.2006.11.004.

Reynolds, R. W., & D. B. Chelton (2010). Comparisons of Daily Sea Surface Temperature Analyses for 2007–08. *J. Clim.*, *23*, 3545-3562, doi:10.1175/2010JCLI3294.1.

Richter, I., S. K. Behera, Y. Masumoto, B. Taguchi, N. Komori, & T. Yamagata (2010). On the triggering of Benguela Niños: Remote equatorial versus local influences. *Geophys. Res. Lett.*, *37*, L20604, doi:10.1029/2010GL044461.

Richter, I., S. K. Behera, Y. Masumoto, B. Taguchi, H. Sasaki, & T. Yamagata (2013). Multiple causes of interannual sea surface temperature variability in the equatorial Atlantic Ocean, *Nat. Geosci*., *6 (1)*, 43–47, doi:10.1038/ngeo1660.

Rouault, M., S. Illig, C. Bartholomae, C. J. C. Reason, & A. Bentamy (2007). Propagation and origin of warm anomalies in the Angola Benguela upwelling system in 2001. *J. Mar. Syst*., *68*, 477-488.

Rouault, M., J. Servain, C. J. R. Reason, B. Bourlès, M. Rouault, & N. Fauchereau (2009). Extension of PIRATA in the tropical South-East Atlantic: an initial one-year experiment. *Afr. J. Mar. Sci*., *31*(1), 63–71, doi:10.2989/AJMS.2009.31.1.5.776.

Rouault, M., S. Illig, J. F. Lübbecke, & R. A. Imbol Koungue (2017). Origin, development and demise of the 2010-2011 Benguela Niño. *J. Mar. Syst.*, doi:10.1016/j.jmarsys.2017.07.007.

Rousselot, P., G. Reverdin, P. Blouch, & P. Poli (2017). *AtlantOS EU H2020 633211 Deliverable 3.5* "Enhancement of autonomous observing networks: Study of the potential for existing bathythermic string drifters" (https://www.atlantos-h2020.eu/project-information/work-packages/deliverables/).

Rugg, A., G. R. Foltz, & R. C. Perez (2016). Role of mixed layer dynamics in tropical North Atlantic interannual sea surface temperature variability. *J. Clim.*, *29*, 8083-8101, doi:10.1175/JCLI-D-1500867.1.

Saha, S., S. Moorthi, H. Pan, X. Wu, J. Wang, S. Nadiga, et al. (2010). Supplement to the NCEP climate forecast system reanalysis. *Bull. Am. Meteorol. Soc., 91*:1015–1057.

Sandel,V., R. Kiko, P. Brandt, M. Dengler, L. Stemmann, P. Vandromme, et al. (2015). Nitrogen Fuelling of the Pelagic Food Web of the Tropical Atlantic. *PLoS ONE 10(6)*: e0131258. doi:10.1371/journal.pone.0131258.

Scannell, H. A. & M. J. McPhaden (2018): Seasonal mixed layer temperature balance in the southeastern tropical Atlantic. *J. Geophys. Res*.: *Ocean*, *123*. https://doi.org/10.1029/2018JC014099.

Schiller, A., F. Davidson, P. M. DiGiacomo, & Wilmer-Becker (2016). Better Informed Marine Operations and Management: Multidisciplinary Efforts in Ocean Forecasting Research for Socioeconomic Benefit, *Bull. Am. Meteorol. Soc.*, doi:10.1175/BAMS-D-15-00102.1.

Schlundt, M., P. Brandt, M. Dengler, R. Hummels, T. Fischer, K. Bumke, & al. (2014). Mixed layer heat and salinity budgets during the onset of the 2011 Atlantic cold tongue. *J. Geophys. Res*., *119*, 7882-7910, doi:10.1002/2014JC010021.

Schmidtko, S., L. Stramma, & M. Visbeck (2017). Decline in global oceanic oxygen content during the past five decades, *Nature, 542*, 335–339, doi:10.1038/nature21399.

Schott, F.A., J. P. McCreary, & G. C. Johnson (2004). Shallow overturning circulations of the tropical–subtropical oceans. In: Wang C, Xie S-P, Carton JA (eds) Earth climate: The ocean–atmosphere interaction. *Geophys. Monogr. 147. American Geophysical Union*, Washington, DC, 261–304.

Schütte, F., J. Karstensen, G. Krahmann, H. Hauss, B. Fiedler, P. Brandt, et al. (2016). Characterization of dead-zone eddies in the eastern tropical North Atlantic, *Biogeosciences*, *13*, 5865–5881, doi:10.5194/bg-13-5865-2016.

Serra, Y.L. & M.J. McPhaden (2003). Multiple time space comparisons of ATLAS buoy rain gauge measurements to TRMM satellite precipitation measurements. *J. Appl. Meteorol.*, *42*, 1045–1059.

Servain J., A. Busalacchi, M. J. McPhaden, A. D. Moura, G. Reverdin, M. Vianna, & S. Zebiak (1998). A Pilot Research Moored Array in the Tropical Atlantic (PIRATA). *Bull. Amer. Meteorol. Soc.*, *79*, 2019-2031, doi:10.1175/1520-0477.

Servain, J., G. Caniaux, Y. K. Kouadio, M. J. McPhaden, & M. Araujo (2014). Recent climatic trends in the tropical Atlantic. *Clim. Dyn*., *43* (11), 3071-3089, doi:10.1007/s00382-014-2168-7.

Shannon, L. V., A. J. Boyd, G. B. Bundrit, & J. Taunton-Clark (1986). On the existence of an El Niño–type phenomenon in the Benguela system. *J. Mar. Syst.*, *44*, 495–520.

Silva, M., M. Araujo, J. Servain, P. Penven, & C.A.D. Lentini (2009). High-resolution regional ocean dynamics simulation in the southwestern tropical Atlantic. *Ocean Modell.*, *30*, 256–269.

Smyth, W. D., J. N. Moum, L. Li, & S.A. Thorpe (2013). Diurnal shear instability, the descent of the surface shear layer, and the deep cycle of equatorial turbulence. *J. Phys. Oceanogr*., *43*, 2432-2455, doi:10.1175/JPO-D-13-089.1.

Stramma, L., G. C. Johnson, J. Sprintall, & V. Mohrholz (2008). Expanding Oxygen-Minimum Zones in the Tropical Oceans, *Science*, *320*, 655–658, doi:10.1126/science.1153847.

Tang, W., S. H. Yueh, A. G. Fore, & A. Hayashi (2014). Validation of Aquarius sea surface salinity with in situ measurements from Argo floats and moored buoys. *J. Geophys. Res. Oceans*, *119*, 6171–6189, doi:10.1002/2014JC010101.

Thierry, V., A. M. Treguier, & H. Mercier (2004). Numerical study of the annual and semi-annual fluctuations in the deep equatorial Atlantic Ocean. *Ocean Modell.*, *6*, 1-30.

Tonani, M., M. Balmaseda, L. Bertino, E. Blockley, G. Brassington, F. Davidson, et al. (2015). Status and future of global and regional ocean prediction systems, *J. Operation. Oceanogr.*, *8 (sup2)*, s201-s220, 10.1080/1755876X.2015.1049892.

Trolliet, M., J. Walawender, B. Bourlès, A. Boilley, J. Trentmann, P. Blanc, et al. (2018). Downwelling surface solar irradiance in the tropical Atlantic Ocean: a comparison of re-analyses and satellite-derived data sets to PIRATA measurements, *Ocean Sciences*, *14*, 1021-1056, https://doi.org/10.5194/os-14-1021-2018.

Tzortzi, E., S. A. Josey, M. Srokosz, & C. Gommenginger (2013). Tropical Atlantic salinity variability: New insights from SMOS. *Geophys. Res. Lett*., *40*, 1-5, doi:10.1002/grl.50225.

Urbano, D. F., M. Jochum, & I. C. A. Silveira (2006), Rediscovering the second core of the Atlantic NECC, *Ocean Modell.*, *12*, 1-15, doi:10.1016/j.ocemod.2005.04.003.

Urbano, D. F., R. A. F. De Almeida, & P. Nobre (2008). Equatorial Undercurrent and North Equatorial Countercurrent at 38°W: A new perspective from direct velocity data, *J. Geophys. Res*., *113*, C04041, doi:10.1029/2007JC004215.

Valdivieso, M., K. Haines, M. Balmaseda, et al. (2017). An assessment of air–sea heat fluxes from ocean and coupled reanalyses. *Clim. Dyn*., *49*, 983-1008, doi:10.1007/s00382-015-2843-3.

Vinogradova, N. T. & R.M. Ponte (2012). Assessing temporal aliasing in satellite-based surface salinity measurements. *J. Atmos. Oceanic Techn*., *29*, 1391-1400, doi:10.1175/JTECH-D-11-00055.1.

Von Schuckmann, K., P. Brandt, & C. Eden (2008). Generation of Tropical Instability Waves in the Atlantic Ocean, *J. Geophys. Res*., *113*, C08034, doi:10.1029/2007JC004712.

Von Schuckmann, K., P.-Y. Le Traon, E. Alvarez-Fanjul, L. Axell, M. Balmaseda, L. et al. (2016). The Copernicus Marine Environment Monitoring Service Ocean State Report, *J. Operation. Oceanogr*., *9 (sup2)*, s235-s320, 10.1080/1755876X.2016.1273446.

Wade, M., G. Caniaux, & Y. duPenhoat (2011). Variability of the mixed layer heat budget in the eastern equatorial Atlantic during 2005-2007 as inferred using Argo floats. *J. Geophys. Res*., *116*, C0800, doi:10.1029/2010JC006683.

Wang, H., & R. T. Pinker (2009). Shortwave radiative fluxes from MODIS: Model development and implementation. *J. Geophys. Res.*, *114*, D2021, doi:10.1029/2008JD010442.

Wang, W. M., & M. J. McPhaden (1999). The surface-layer heat balance in the equatorial Pacific Ocean. Part I: mean seasonal cycle. *J. Phys. Oceanogr., 29*, 1812–1831.

Wenegrat, J. O., M. J. McPhaden, & R.-C. Lien (2014). Wind stress and near-surface shear in the equatorial Atlantic Ocean. *Geophys. Res. Lett*., *41*, 1226–1231, doi:10.1002/2013GL059149.

Wenegrat, J. O., & M. J. McPhaden (2015). Dynamics of the surface layer diurnal cycle in the equatorial Atlantic Ocean (0, 23W). *J. Geophys. Res. Oceans*, *120*, doi:10.1002/2014JC010504.

Woodruff, S. D., S. J. Worley, S. J. Lubker, Z. Ji, J. E. Freeman, D. I. Berry, et al. (2011). ICOADS Release 2.5: extensions and enhancements to the surface marine meteorological archive. *Int. J. of Clim., 31*, 7, 951-967, doi:10.1002/joc.2103.

Wu, Q., and K. P. Bowman (2007), Interannual variations of tropical instability waves observed by the Tropical Rainfall Measuring Mission, *Geophys. Res. Lett., 34*, L09701, doi:10.1029/2007GL029719.

Xie, P., R. Joyce, S. Wu, S. Yoo, Y. Yarosh, F. Sun, & R. Lin (2017). Reprocessed, Bias-Corrected CMORPH Global High-Resolution Precipitation Estimates from 1998. *J. Hydrometeor., 18*, 1617–1641, doi:10.1175/JHM-D-16-0168.1.

Xu, Z., M. Li, C.M. Patricola, & P. Chang (2014). Oceanic origin of southeast tropical Atlantic biases. *Clim. Dyn., 43*, 2915–2930

Xue, Y., C. Wen, A. Kumar, M. Balmaseda, Y. Fujii et al. (2017). A real-time ocean reanalyses intercomparison project in the context of tropical pacific observing system and ENSO monitoring, *Clim. Dyn*., *49* (11), 3647-3672, doi:10.1007/s00382-017-3535-y.

Yu, L., & R. A. Weller (2007). Objectively Analyzed air-sea heat Fluxes (OAFlux) for the global ice-free oceans. *Bull. Amer. Meteor. Soc*., *88(4*), 527-539, doi:10.1175/BAMS-88-4-527.

Yu, L., & X. Jin (2012). Buoy perspective of a high-resolution global ocean vector wind analysis constructed from passive radiometers and active scatterometers (1987–present*). J. Geophys. Res*., *117*, C11013, doi:10.1029/2012JC008069.

Zhang, D., M. J. McPhaden, & W. E. Johns (2003). Observational evidence for flow between the subtropical and tropical Atlantic: The Atlantic subtropical cells. *J. Phys. Oceanogr*., *33*, 1783–1797.

Zhu, J., B. Huang, & Z. Wu (2012). The Role of Ocean Dynamics in the Interaction between the Atlantic Meridional and Equatorial Modes. *J. Climate*, *25*, 3583–3598, doi:10.1175/JCLI-D-11-00364.1.

Zuidema, P., P. Chang, B. Medeiros, B. Kirtman, R. Mechoso, E. Schneider, et al. (2016). Challenges and Prospects for Reducing Coupled Climate Model SST Biases in the Eastern Tropical Atlantic and Pacific Oceans: The U.S. CLIVAR Eastern Tropical Oceans Synthesis Working Group. *Bull. Amer. Meteor*. *Soc*., *97*, 2305–2327, doi:10.1175/BAMS-D-15-00274.1.

Zuo, H., M. A. Balmaseda, & K. Mogensen (2017). The new eddy-permitting ORAP5 ocean reanalysis: description, evaluation and uncertainties in climate signals. *Clim. Dyn*. *49*, 791–811, doi:10.1007/s00382-015-2675-1.

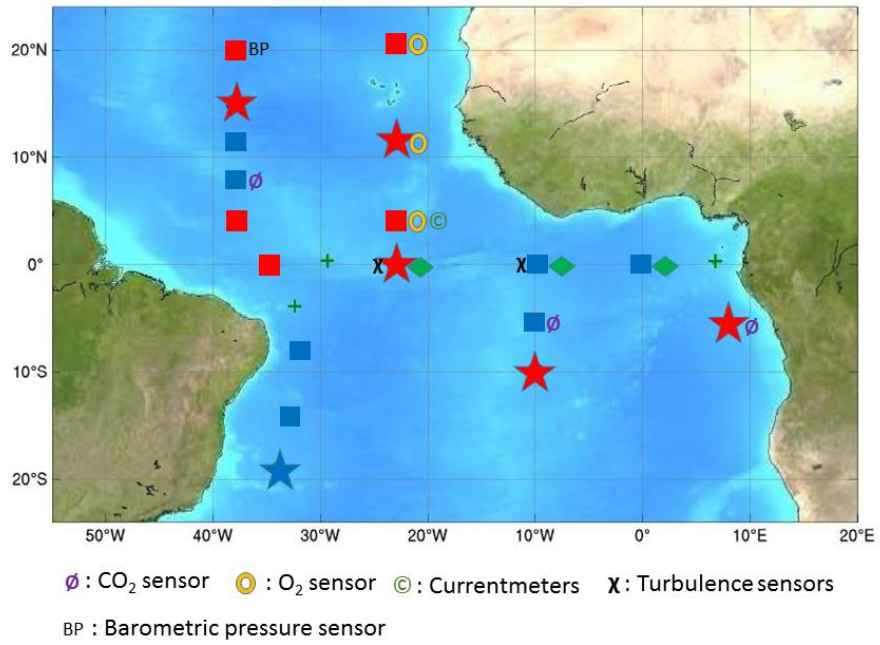

Figure 1: The present PIRATA network: the meteo-oceanic buoys are represented by rectangles and by stars for Flux Reference Sites. T-Flex moorings are colored in red and ATLAS moorings in blue. ADCP moorings are represented by green diamonds. Additional symbols are explained in the map legend. All meteo-oceanic buoys are equipped with OTN. Green crosses represent some island-based observation sites (i.e. tide gauges and meteorological stations; see Bourlès et al., 2008).

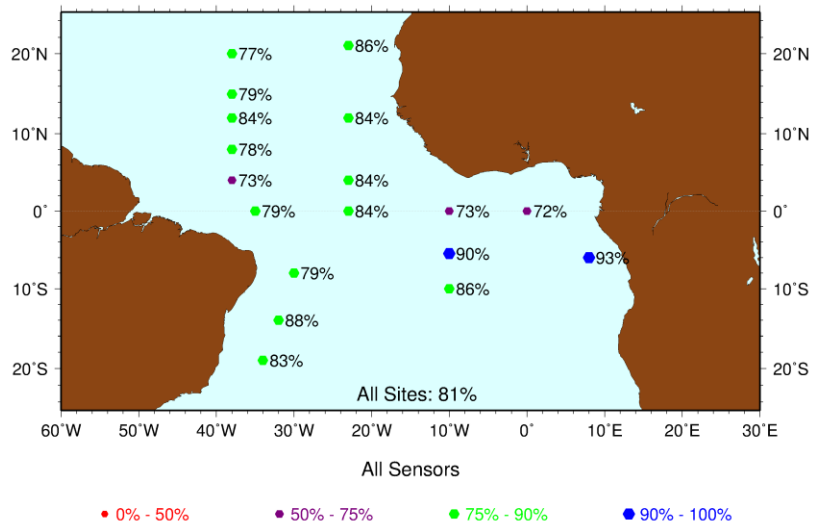

Figure 2: The overall PIRATA buoys delayed mode data return over the 1997-2017 period, mean value for all sensors at each moored location.

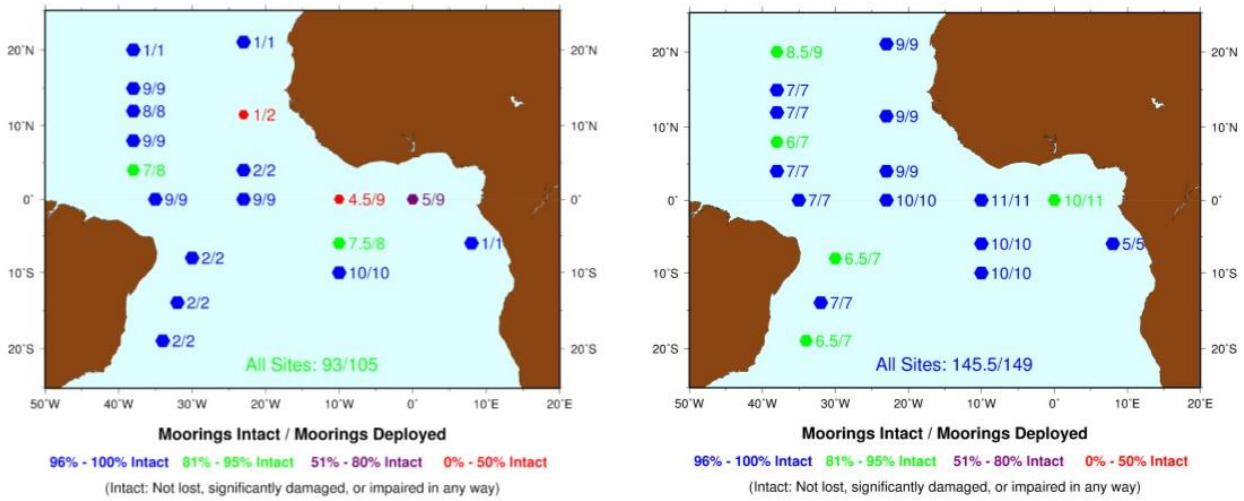

Figure 3: PIRATA mooring survival over the 1997-2007 (left) and 2008-2017 (right) periods.

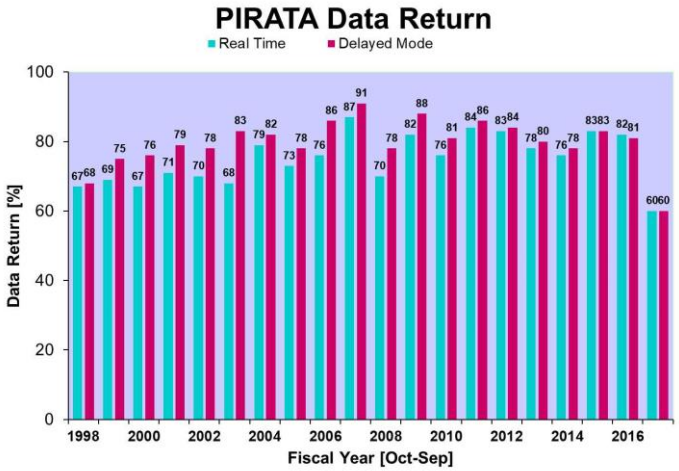

Figure 4: Annual PIRATA moorings data return evolution from 1997 to 2017: real time (delayed mode) data return are represented by blue (red) bars respectively.

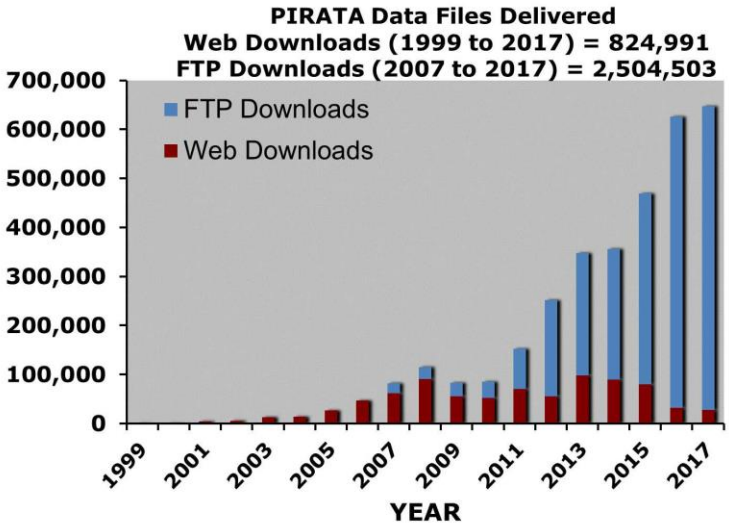

Figure 5: Annual PIRATA data files delivered from 1999 to 2017: ftp (web) data downloads are represented by blue (brown) bars respectively.

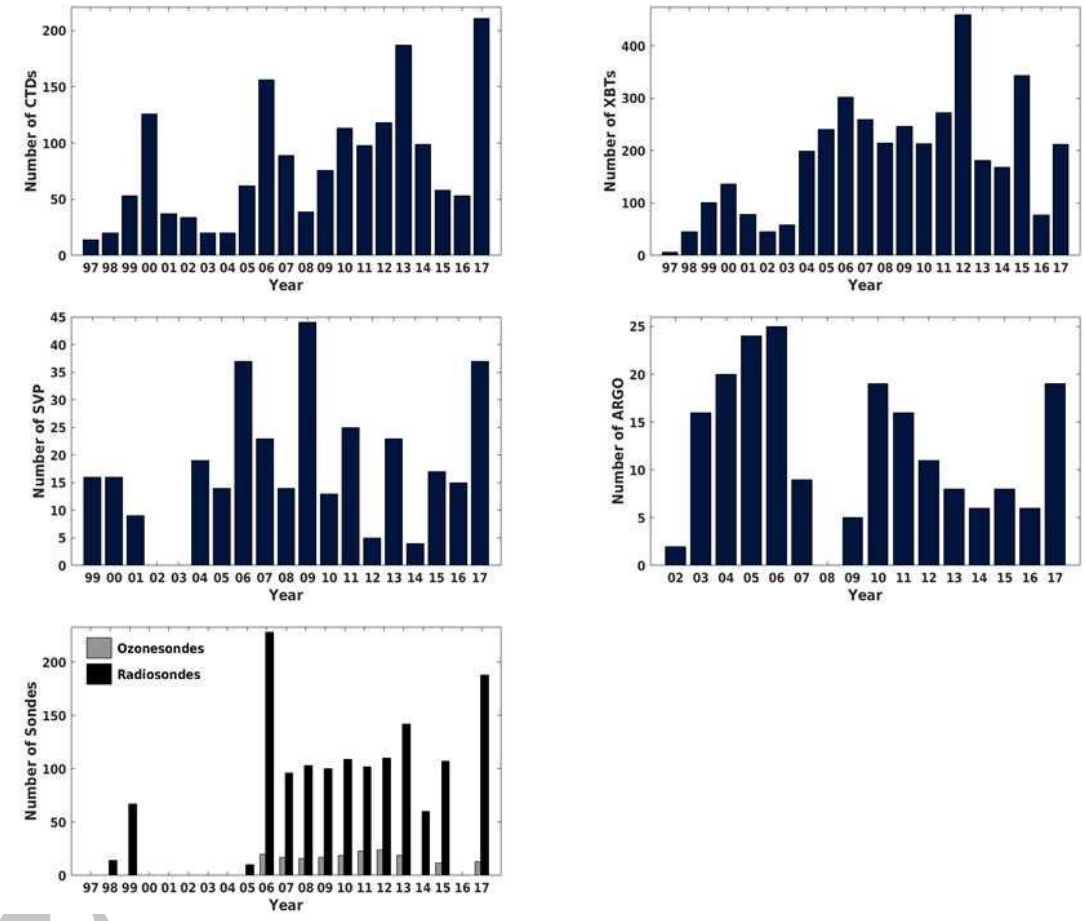

Figure 6: Number of deployed CTD (upper left), XBT (upper right), SVP (middle left), Argo profilers (middle right), radiosondes and ozonesondes (bottom) during PIRATA cruises from 1997 to 2017.

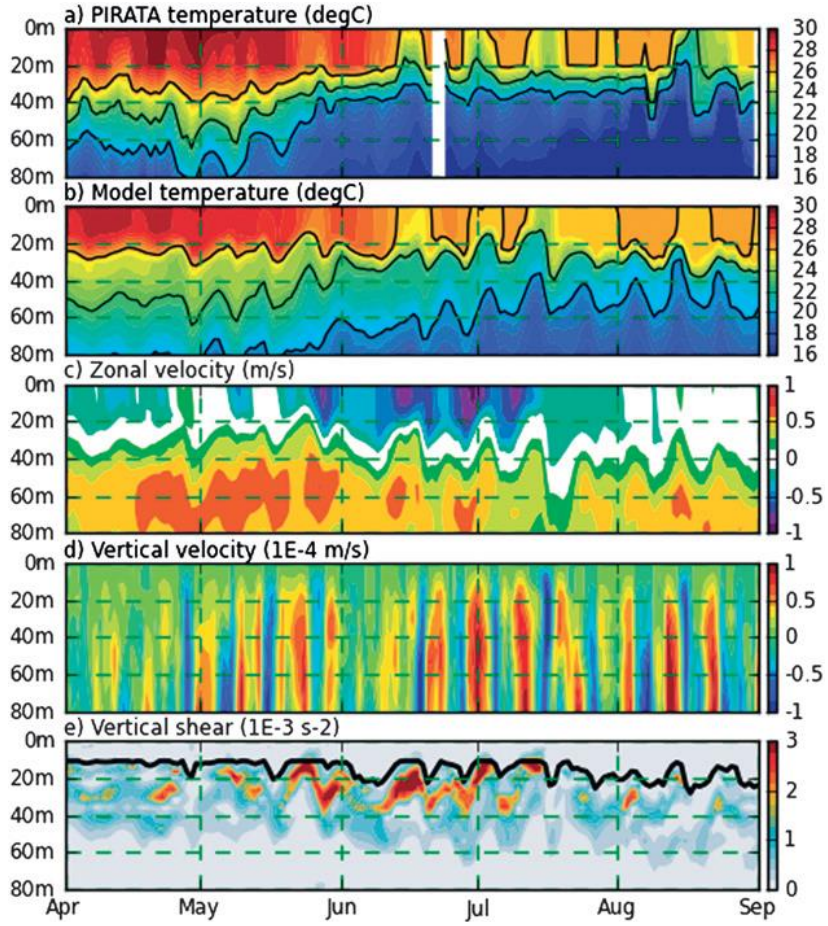

Figure 7: Time–depth diagrams at 0°, 0° of:
(a) Observed PIRATA temperature (°C), (b) model temperature (°C), (c) model zonal velocity (m s^{-1}), (d) model vertical velocity (10^{-4} m s^{-1}), and (e) vertical shear of horizontal velocities (10^{-3} s^{-2}).
Black lines represent the 20°, 23°, and 26°C isotherms in (a), (b) and the depth of the model mixed layer in (e). Data are shown from April to August 2007. From Jouanno et al. (2013), their Figure 16 (reprinted by permission from American Meteorological Society).

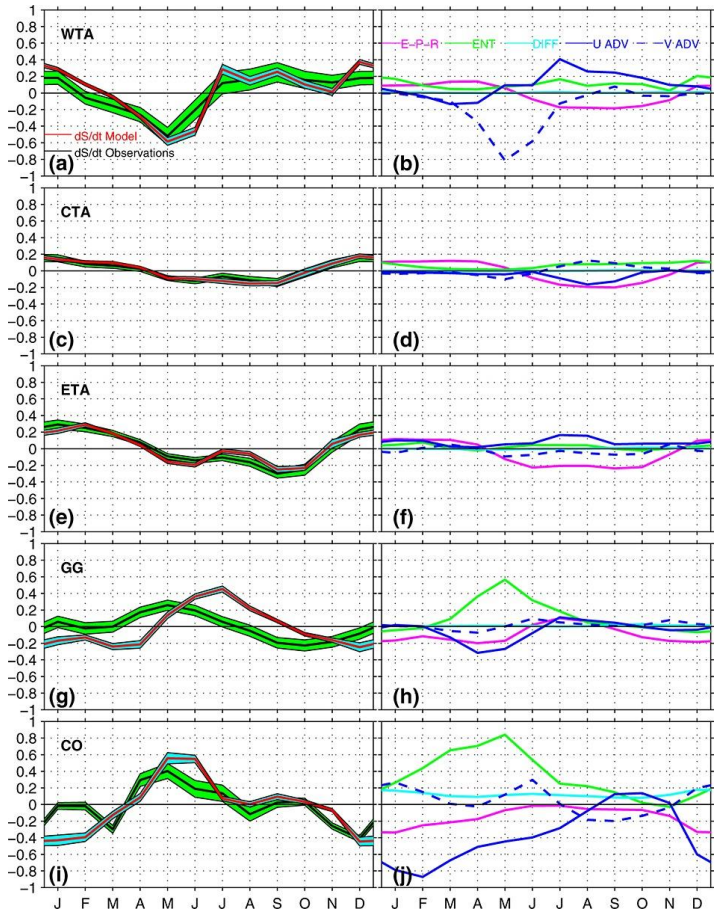

Figure 8:
a, c, e, g, and i: Salinity tendency terms in the mixed layer for five selected regions with the shaded areas indicating error estimates for these two terms; b, d, f, h, and j: Individual contributions to the salt balance equation of freshwater flux (purple), entrainment (green), horizontal diffusion (light blue), zonal advection (blue), and meridional advection (dashed blue). All terms are given in month^{-1}. The five selected regions are: a, b) WTA for Western Tropical Atlantic; c, d) CTA for Central Tropical Atlantic; e, f) ETA for Eastern Tropical Atlantic; g, h) GG for Gulf of Guinea; i, j) CO for Congo Region. From Da-Allada et al. (2013), their Figure 13 (reprinted by permission from American Geophysical Union).

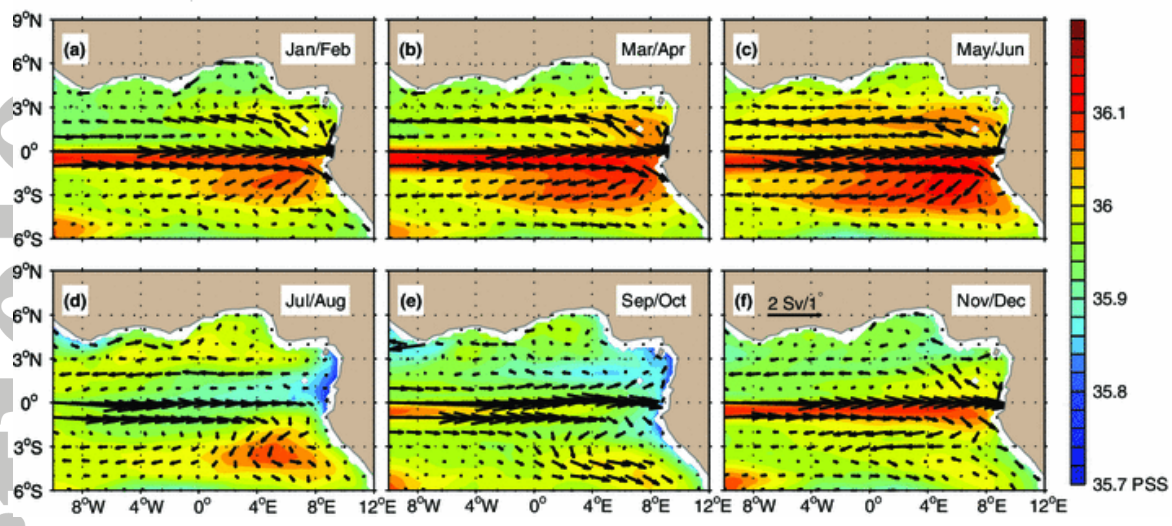

Figure 9: Bi-monthly climatology of the transport per unit of latitude/longitude (arrows; scaling provided in the bottom/right panel) and mean salinity (shaded color) in the 24.5–26.2 isopycnal layer, as inferred from the Ocean General Circulation Model NEMO. Months from January/February (a) to November/December (f) are indicated, from top/left to bottom/right, in each panel. From Kolodziejczyk et al. (2014), their Figure 11 (reprinted by permission from Springer Nature, Licence Number 4533541196832).

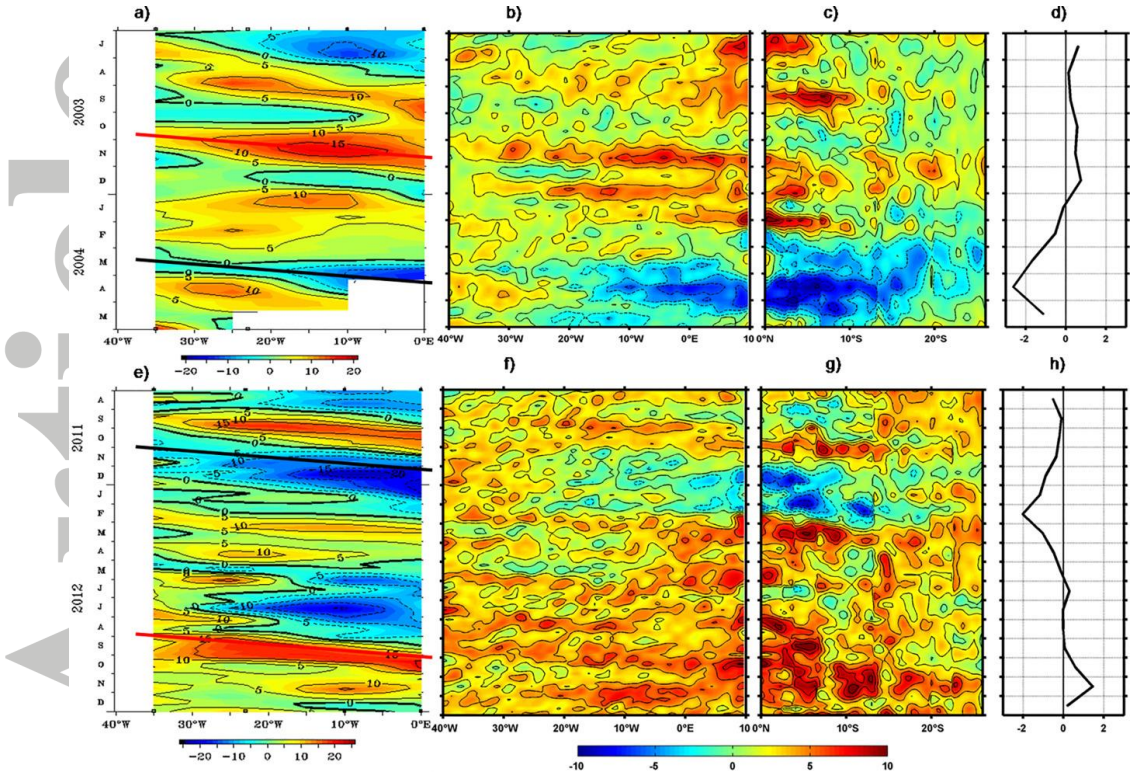

Figure 10: Top: from left to right, a) longitude-time diagram of 5 day means of Z20 anomalies (m) along the equator inferred from PIRATA moorings and interpolated between mooring locations, (b) SSH anomalies (cm) inferred from AVISO along the equator averaged between 18°S and 18°N, (c) latitude-time diagram of SSH anomalies (cm) inferred from AVISO averaged within 18 coastal fringe, and (d) time series of SST anomalies (°C) averaged from 10°S to 15°S within 18 coastal fringe for the period July 2003 to May 2004. Bottom, e, f, g, h: The same plots are represented, but for the period August 2011 to December 2012. The red and black tick straight lines represent eastward phase speed estimates (m/s). From Imbol Koungue et al. (2017), their Figure 4 (reprinted by permission from American Geophysical Union).

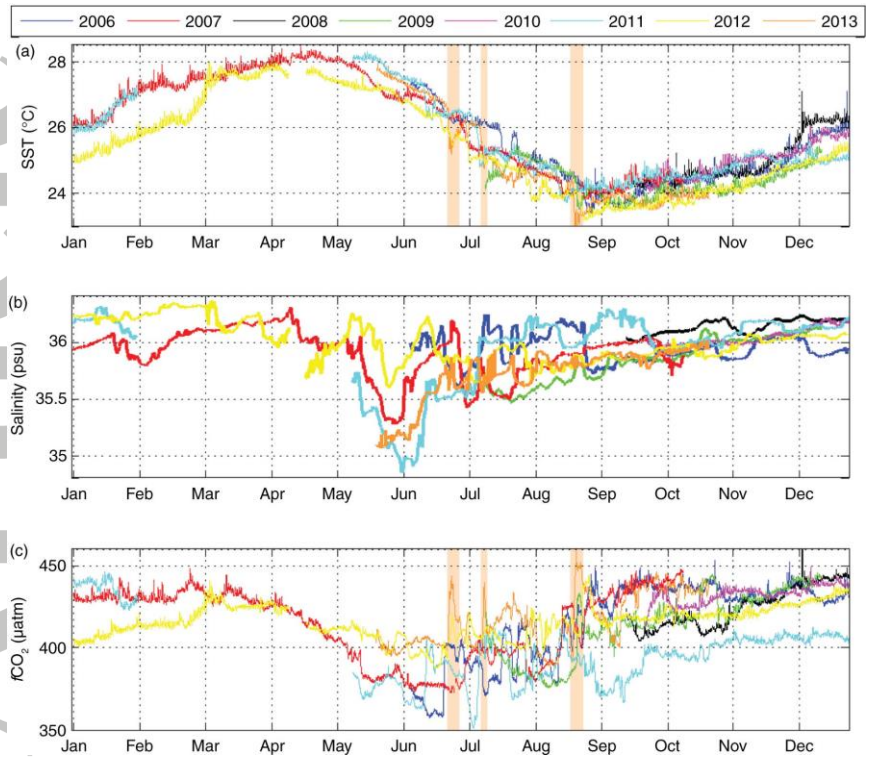

Figure 11: Hourly distribution of (a) SST, (b) SSS and (c) fCO_2 at the PIRATA buoy located at 6°S-10°W from January to December for the years 2006 to 2013. From April 2012 the high resolution SSS is not available so mean daily data are plotted. Orange shaded areas correspond to high fCO_2 associated with low SST. From Lefevre et al. (2016), their Figure 3 (reprinted by permission from Taylor and Francis Group).

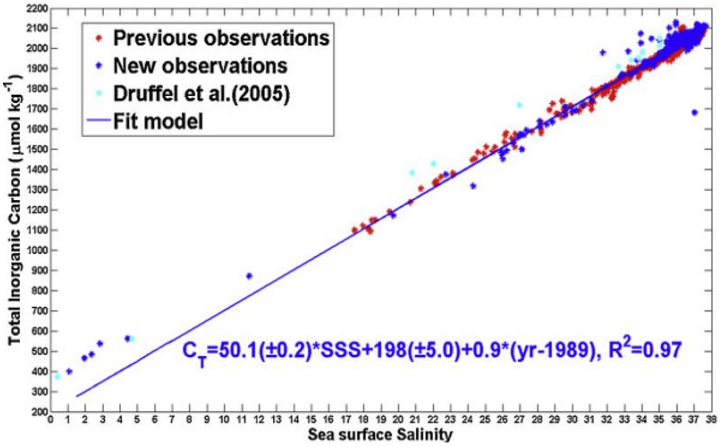

Figure 12: Sea surface total inorganic carbon as a function of SSS, as obtained from several sets of in situ data. The blue line corresponds to a fit using all the data. New observations refer to in situ measurements obtained from 35 cruises in the western tropical Atlantic realized from 1989 to 2014. From Bonou et al. (2016), their Figure 6b (reprinted by permission from Elsevier, Licence Number 4533681278066).

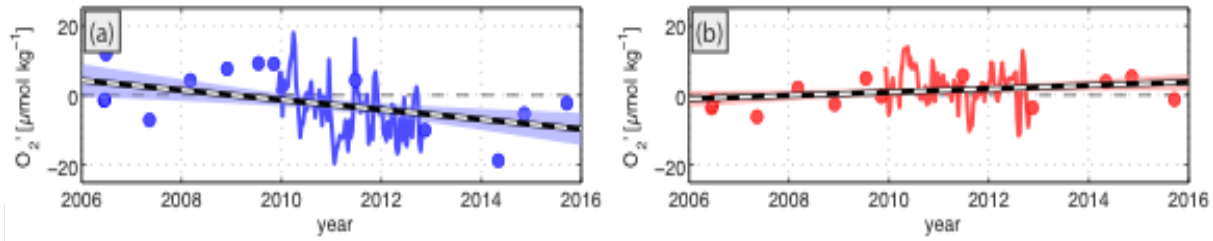

Figure 13: Oxygen anomaly time series from moored (solid line) and shipboard (dots) observations at 8°N-23°W, a) averages between 200 and 400 m, b) averages between 500 and 800 m. Black dashed lines show respective trends from combined moored and shipboard observations: (a) -13.9±8.7 µmol kg^{-1} decade^{-1}, (b) 4.8±4.4 µmol kg^{-1} decade^{-1}. From Hahn et al. (2017), their Figure 4 (reprinted by permission from European Geophysical Union).

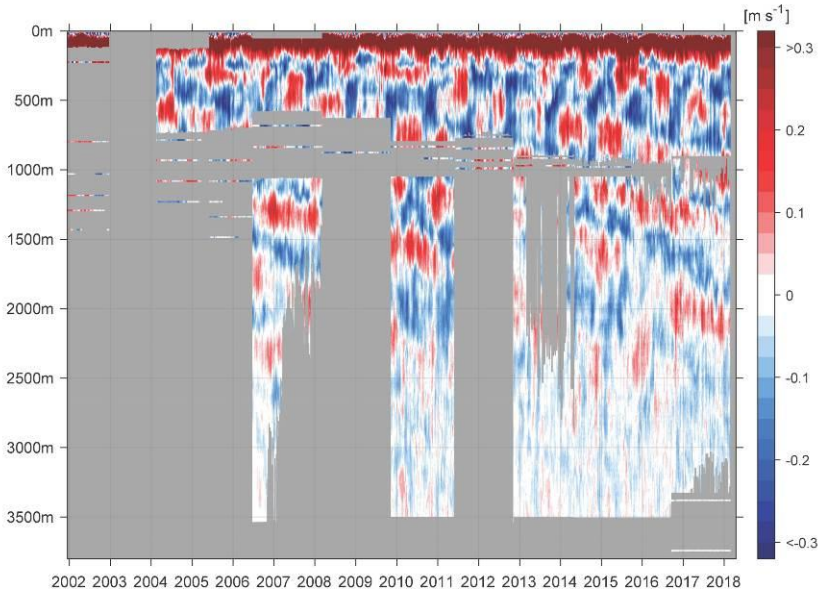

Figure 14: Zonal velocity ($m.s^{-1}$) at the equator 23°W as inferred from moored measurements from 2001 to 2018 (courtesy P. Brandt, update from Brandt et al. 2011b).

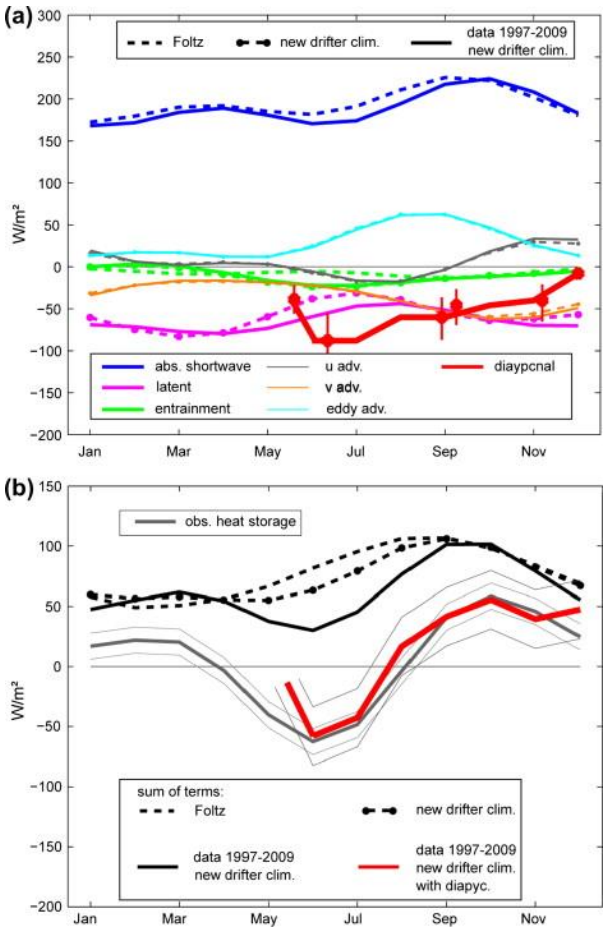

Figure 15:
a) Individual terms of the ML heat budget at 10°W,0°N: dashed lines are a reproduction of the Foltz et al. (2003) estimates with coarse drifter resolution, using data from 1997–2002; dashed-dotted lines indicate advective and eddy heat flux estimates from the period 1997–2002 using a drifter climatology of higher resolution compared to the climatology used by Foltz et al. (2003); solid lines indicate flux estimates using the higher resolution drifter data and data from the time period 1997–2009; the red bars denote confidence limits for the average diapycnal heat flux below the ML; b) black lines represent the sum of all terms contributing to the heat budget except turbulent heat flux (line styles are assigned to the same set ups as in (a)), red line indicates sum of all terms including diapycnal heat flux. From Hummels et al. (2013), their Figure 16 (reprinted by permission from Elsevier, Licence Number 4533661391935).

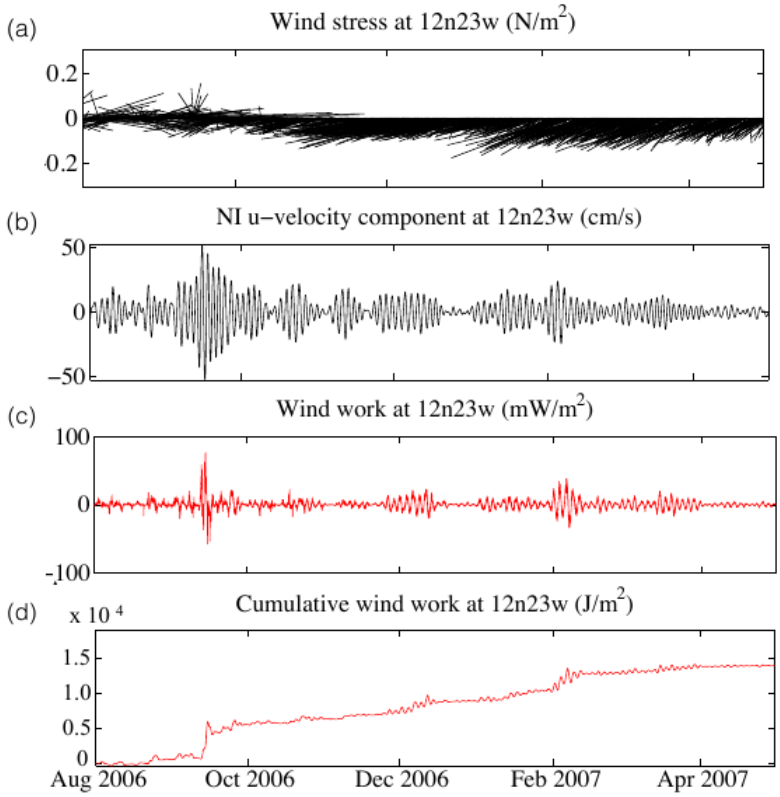

Figure 16: Analysis of surface wind stress and 10m depth ocean velocity at the 12°N-23°W PIRATA mooring (courtesy H. Pillar).

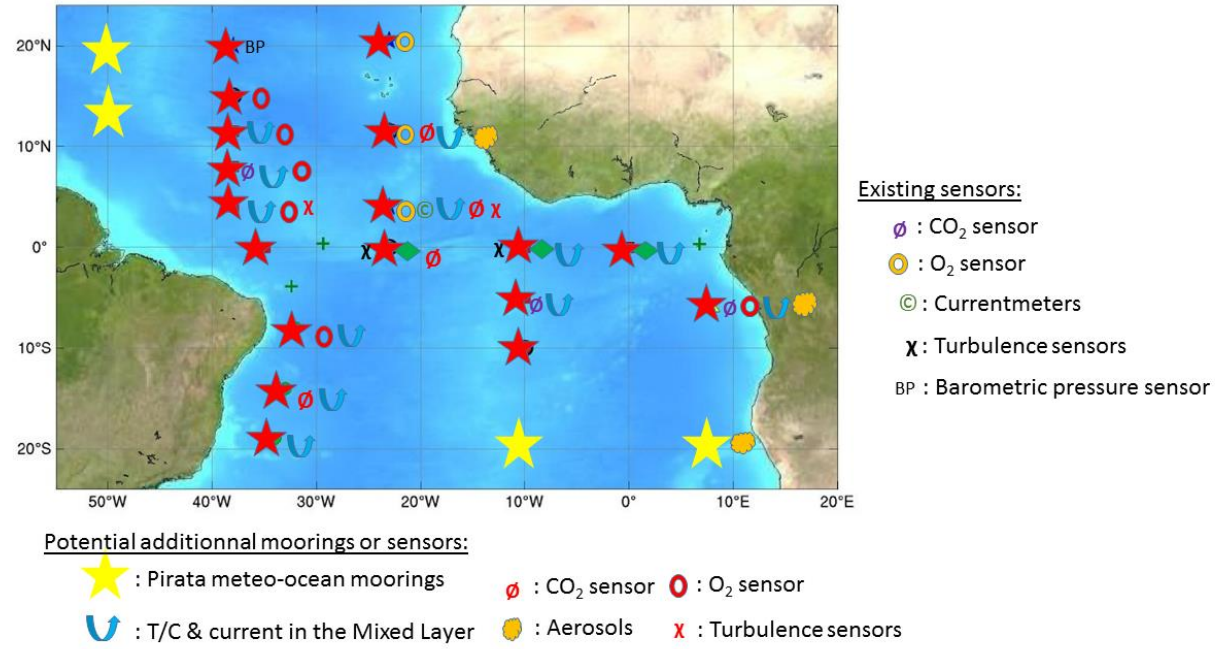

Figure 17: Possible enhancements and extensions of the PIRATA network.

Table 1: List of measurement operations carried out during dedicated PIRATA cruises and by each partner country (FR: France; BR: Brazil; US: USA). Adapted from Bourlès et al. (2017).

		FR cruises	BR cruises	US cruises
Vertical profiles	**CTD or CTDO$_2$ / depth / quasi real time data transmission (qrtdt)**	CTDO$_2$; 0-2000m; qrtdt	CTD; 0-1500m; CTDO$_2$ full depth from 2017 ; qrtdt	CTDO$_2$; 0-1500m; qrtdt
	L-ADCP	Yes; 0-2000m	Yes; 0-1500m ; full depth from 2017	Yes; 0-1500m
	Bottle S analysis	Yes; 0-2000m	Yes; 0-1500m ; full depth from 2017	Yes; 0-1500m
	Bottle O2 analysis	Yes; 0-2000m	Yes : 0-1500m ; full depth from 2017	Yes; 0-1500m
	Bottle nutrients analysis	Yes; Nitrates, Nitrites, Phosphates, Silicates 0-2000m	Yes ; full depth from 2017	No
	Bottle Chl pigments analysis	Yes ; 0-100m	No	No
	Bottle inorganic carbon parameters	only at CO$_2$ equipped buoys ; 0-100m	only at CO$_2$ equipped buoys ; 0-100m	No
	XBT or XCTD / depth / quasi real time data transmission (qrtdt)	XBT; 0-800m; qrtdt	XBT; 0-800m; qrtdt	XBT; 0-800m; qrtdt
Continuous measurements	**SST&SSS (Tsgraph)**	Yes	Yes	Yes
	S-ADCP	Yes	Yes	Yes
	Surface ocean & atmosphere CO$_2$ fugacity	No	Yes	Yes (usually; not always)
	Acoustic EK60/80	Yes (from 2015; RV Thalassa)	Yes, (only with RV Vital de Oliveira)	No
	Meteo	Yes	Yes	Yes
	U-CTD	No	Yes	No
Opportunity	**Argo profilers**	Yes (about 7 per cruise)	Yes (from 2017)	Yes

operations				
	Surface drifters	Yes; SVP or SVP-S & BS (number depending of years)	Yes; SVP (number depending of years)	Yes
	Radiosoundings	No	Yes (number depending of years)	Yes (usually; not always)
	Aerosols	No	Yes (from 2017 with RV vital de Oliveira)	Yes
	O3 (ozonesondes)	No	No	Yes (usually; not always)

Cross correlation	Buoy at 8°S-30°W	Buoy at 19°S-34°W
SAT.SST	**0.91**	**0.94**
SWR.PREC	**-0.64**	**-0.74**
SAT.SWR	*-0.38*	*0.49*
SST.SWR	-0.18	*0.41*
SAT.PREC	*0.56*	-0.32
SST.PREC	0.33	-0.19

*Table 2: Anomaly cross correlation between surface air temperature (SAT), sea surface temperature (SST), Rainfall (PREC), and downward shortwave radiation (SWR) for the PIRATA buoys at 8°S-30°W and 19°S-34°W. Daily values smoothed with a 30-day running mean filter for the December-to-February periods of the years 2005 to 2010, totaling 450 pairs of data for each time series. Cross correlation values greater than 0.35 (**0.6**) are statistically significant at the 90% (**99%**) significance level according to one-sided student-t test with 15 degrees of freedom. From Nobre et al. (2012).*